Latvijas Universitātes aģentūra

Latvijas Universitātes
Fizikas Institūts

Renovētā sārmu metālu laboratorija

Publiskais pārskats

2009.gads

Misija

Latvijas Universitātes Fizikas institūta (LU FI) misija ir iedibināta vēsturiski: zinātniskie pētījumi magnētiskajā hidrodinamikā (MHD) un ar to saistītās zinātnes nozarēs un ar to saistītu pielietojumu realizēšana un arī jauno speciālistu sagatavošanu šajās zinātnes nozarēs. LUFI darbojas kopējies Latvijas Universitātes misijas kontekstā.

Latvijas Universitātes Fizikas institūta īsa vēsture.

LU FI atrodas Salaspilī, Miera ielā 32. dibināts 1946.g. kā Latvijas PSR ZA Fizikas un matemātikas institūts, no 1950.gada Latvijas ZA Fizikas institūts, Latvijas Universitātes Fizikas institūts kopš 1997.

Direktori: 1946-1948 N.Brāzma ; 1948-1967 I.Kirko; 1967-1991 J.Mihailovs; 1992-1993 I.Bērsons; 1994-1997 O.Lielausis; 1998-2000 A.Gailītis.

Kopš 2001.g. direktors ir J.E.Freibergs. Zinātniskās padomes priekšsēdētājs A.Gailītis. Akadēmiskais personāls pašlaik ir 48 (asistenti, pētnieki un vadošie pētnieki), no tiem 6 habilitētie dokt., 35 doktori.

2006. gada 1. maijā LU Fizikas institūts atbilstoši Likumam par zinātnisko darbību tika reorganizēts par LU aģentūru.

LU FI darbības 2009.gada pamatmērķi ir sekojoši:

- Uzturēt LU FI kā vadošo pētniecības centru magnētiskajā hidrodinamikā un ar to saistītās zinātnēs gan Latvijā, gan Eiropā un izveidot LU FI par atzītu pētniecības iestādi Pasaules zinātniskajā telpā.
- Uzlabot sadarbību ar LU Fizikas un matemātikas fakultāti zinātnē un jauno speciālistu audzināšanā un arī ar radniecīgām fakultātēm RTU.
- Pastiprināt sadarbību ar ārzemju zinātniekiem jo sevišķi ar Francijas zinātniekiem, kā arī ar Vācijas, Lielbritānijas un Nīderlandes zinātniekiem. Veiksmīgi uzsākta sadarbība ar Indijas zinatniekiem
- Turpināt strādāt pie **Ampēra iniciatīvas** projekta realizēšanas.

Atbilstība prioritārajiem virzieniem.

Materiālzinātne (nanotehnoloģijas funkcionālo materiālu iegūšanai un jaunas paaudzes kompozītmateriāli);
Enerģētika – videi draudzīgi atjaunojamās enerģijas veidi, enerģijas piegādes drošība un enerģijas efektīva izmantošana.

Lietišķo pētījumu virzieni: šķidro metālu tehnoloģijas jaunas paaudzes kodolreaktoriem un kodolsintēzes reaktoriem (enerģijas ražošanas un piegādes drošība); MHD saules enerģijas pārveidotājs (videi draudzīgi atjaunojamās enerģijas veidi); MHD tehnoloģiju izmantošana jauna veida metālu sakausējumu iegūšanai (materiālzinātne); magnētiskie šķidrumi, magnētiskā lauka izmantošana nanoierīču vadīšanai, magnētisko parādību un kapilāro parādību mijiedarbība (nanotehnoloģijas funkcionālo materiālu un ierīču iegūšanai); starpnozaru pētījumi – magnētiski vadāmu nanoierīču izmantošana biomedicīnā.

Latvijas Universitātes dibināta Latvijas Universitātes aģentūra „Latvijas Universitātes Fizikas institūts”; 17.03.2006.g. Latvijas Universitātes Senāta lēmums Nr.177
Reģistrēts LR VID ar kodu LV90002112199; reģistrēts Nodokļu maksātāju reģistrā ar kodu 90002112199

LR IZM Zinātniskās institūcijas reģistrācijas apliecība Nr.551021

LU Fizikas institūta struktūra

LU FI ir 6 zinātniskās struktūrvienības:
Fizikālās hidromehānikas lab. (vad. E.Platacis), Siltuma un masas pārneses lab. (E.Blūms), MHD tehnoloģijas lab. (A.Bojarēvičs), MHD mašīnu teorijas lab. (A.Šiško), Elektrovirpuļplūsmu lab. (J.Freibergs), Teorētiskās fizikas lab. (A.Gailītis).

Direkcija
Grāmatvedība
Enerģētikas un saimniecības dienests

Vidējais zinātniskā personāla skaits **44,0** 2006 gadā PLE izteiksmē
Vidējais zinātnisko darbinieku skaits **74,0** 2006 gadā PLE izteiksmē

Tālrunis	67944700
Fakss	67901214
E-pasts	fizinst@sal.lv
Internets	http://ipul.lv
Direktors	**Dr.fiz. Jānis Freibergs**
Tālrunis	67944700
Fakss	67901214
E-pasts	jf@sal.lv
Direktora vietnieks	**Dr.fiz. A.Gailītis**
Tālrunis	67945821
e-pasts	gailitis@sal.lv
Direktora palīdze	**Maija Broka**
Tālrunis	67944700
Fakss	67901214
E-pasts	mbroka@sal.lv
Atrodas	Salaspilī, Miera ielā 32
Pasta adrese	Miera ielā 32, Salaspils-1, LV-2169
Sadarbības fakultātes	Fizikas un matemātikas fakultāte
Akadēmiskā personāla skaits (asist., pētn., v.pētn., .) uz 01.01.2009.	**60**
tsk.:	
doktori	**36**
habilitētie doktori	**6**

Kopš 1965. gada LU FI izdod starptautisku žurnālu "Magnētiskā hidrodinamika" (tagad angļu valodā „MagnetoHydroDynamics”, iznāk 4 reizes gadā; galvenais redaktors A.Cēbers).

LU FI organizē regulāras starptautiskas MHD konferences.

Zinātniskā padome

Zinātniskās padomes priekšsēdētājs Dr.phys. A. Gailītis

Dr.hab.phys. E.Blūms

Maģistrs Andris Bojarēvičs

Dr.phys. I. Bucenieks

Dr.phys. L. Buligins

Dr.hab.phys. A.Cēbers

Dr.phys. J.E.Freibergs

Dr.phys. A.Gailītis

Dr.hab.phys. J.Gelfgāts

Dr.phys. A.Mežulis

Dr.hab.phys. O. Lielausis

Dr.phys. I. Grants

Dr.phys. E. Platacis

Dr.phys. M. Zaķe

LUFI zinātniskās pētniecības apakšvirzieni

I apakšvirziens

Zinātniskās pētniecības apakšvirziens, kurā LUFI ir vadošo institūciju vidū pasaulē:

Šķidru metālu magnetohidrodinamika un hidrodinamika, fundamentālie un pielietojumie pētījumi.

Vadošais personāls:
Dr.Phys. I.Bucenieks, J.Freibergs, A.Gailītis; I.Grants, A.Kļukins, O.Lielausis; E.Platacis; I.Platnieks; A.Šiško, Vl.Kremeņeckis

II apakšvirziens

Magnētisko nanokoloīdu fizika

Vadošais personāls:
Dr.hab.phys. E.Blūms, Dr.phys. A. Mežulis, M. Majorovs, G.Kroņkalns.

III apakšvirziens

Degšanas procesu dinamikas izpēte.

Vadošais personāls:
Vad. pētn. Dr. phys. M.Zaķe, Dr. sci. Ing. I.Barmina, Dr.sci.ing. A.Meijere

Latvijas Universitātes aģentūras
„Latvijas Universitātes Fizikas institūts"
darba plāns 2009.gadam

Šis darba plāns ir Latvijas Universitātes (LU) un Latvijas Universitātes Fizikas institūta (LU FI) Pārvaldes līguma pielikums.

LU FI veic savu darbību saskaņā ar savu Nolikumu, Pārvaldes līgumu un savu vidēja termiņa stratēģiju.

LU FI nodrošina savu pētniecisko darbību un publisko pakalpojumu sniegšanu atbilstoši zinātnieku ētikas kodeksam, starptautiski atzītiem labas prakses paraugiem un LU FI iekšējiem normatīviem dokumentiem, tādejādi nodrošinot savas darbības attiecīgos kvalitatīvos rādītājus un ceļot institūta prestižu kopumā.

LU FI nodrošina ar 04.08.2008. Ministru Kabineta noteikumiem Nr. 623 "Bāzes finansējuma piešķiršanas kārtība valsts zinātniskajām institūcijām un valsts augstskolu zinātniskajiem institūtiem" noteiktos zinātnisko institūtu novērtēšanas rādītājus tādā mērā, lai integrētais novērtējums par 2009.gadu nav mazāks par 10.

LU FI 2009.gadam noteiktie kvalitatīvie un kvantitatīvie rādītāji atspoguļoti nākošajā tabulā.

		2009.gadā
Zinātnisko pētījumu tematiskās jomas, kurās institūtam būs nozīmīga loma, saskaņā ar stratēģiju		4
Zinātniskā personāla attīstības rādītāji (skaita pieaugums pret iepriekšējo gadu, %)		1 %
Finansējuma attīstības rādītāji (apjoma pieaugums pret iepriekšējo gadu, %)		15%
Sagatavoto zinātnisko publikāciju skaits		60
tai skaitā:	SCI publikācijas (publikācijas izdevumos, kas tiek referēti starptautiski pieejamās datu bāzēs)	30
	Publikācijas starptautiski recenzētos, LZP atzītos izdevumos	19
	Publikācijas citos zinātniskajos izdevumos	8
	Populārzinātniski raksti	3
Konferenču tēzes		10
Sagatavoto un piedāvāto studiju kursu skaits		2
Sagatavotie laboratorijas darbu komplekti		2
Doktorantiem, maģistrantiem un bakalauriem piedāvāto darba vietu un/vai pētījumu tēmu skaits		6
Starptautiskās atpazīstamības rādītāji (starptautiski nozīmīgi projekti vai pasākumi kopā)		6
Eiropas Savienības.6 un 7.ietvara projektu skaits		5
Valsts pētījumu programmu projektu skaits		2
LZP finansētie sadarbības projekti		3
Latvijas Zinātnes padomes finansēto projektu skaits		4
Reģistrēto un uzturēto patentu skaits		1

LU FI nodrošina institūta darbības nepārtrauktību, balstoties uz iespējamo risku apzināšanu sekojošās sadaļās, bet jo īpašu vērību pievēršot personāla atjaunināšanai un darbinieku kvalifikācijas paaugstināšanai (cilvēku kapitāla riski), finanšu disciplīnas un likumības ievērošanai (finanšu un juridiskie riski), kā arī kvalitatīvai publisko pakalpojumu sniegšanai (darbības riski). Darbības risku pārvaldīšanai LU FI atspoguļo rīcības plānā.

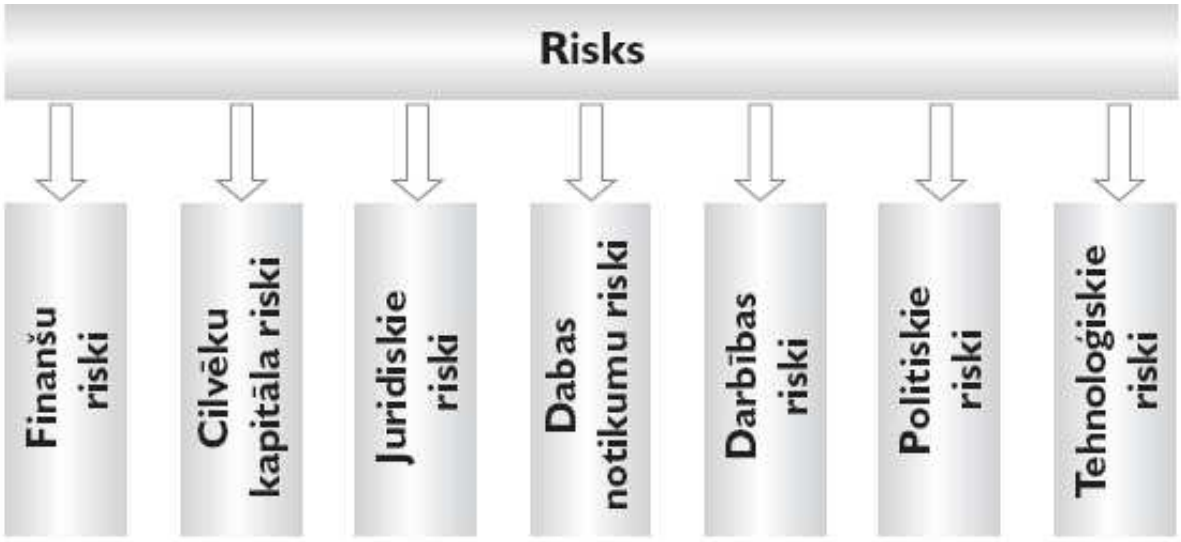

LU FI nodrošina risku identificēšanu un to pārvaldību saskaņā ar sekojošu darba plānu.

Kārtas Nr.	Darbības raksturojums	Izpildes termiņš vai pasākuma biežums
1.	Darba grupas izveide riska faktoru identificēšanai un novērtēšanai LU FI	2. kvartāls
2.	LU FI riska pārvaldības politikas dokumenta izstrāde	2. kvartāls
3.	Pasākumu plāna izstrāde riska faktoru mazināšanai	2.kvartāls
4.	LU FI datu drošības politikas dokumenta uzlabošana	3.kvartāls
4.	Iekšējās kontroles politika dokumenta uzlabošana	3.kvartāls
5.	Riska faktoru pārvērtēšana un pasākumu plāna korekcija 2009.gadam	4.kvartāls

LU Fizikas institūta ieņēmumi 2009.gadā 540,3 tūkstoši latu.

Finansējums kopā (tūkst.Ls ar vienu zīmi aiz komata)	540,3
tai skaitā: **Valsts budžeta finansējums**	371,6
no tā: Eiropas Savienības struktūrfondu finansējums zinātniskajai darbībai	
Latvijas Zinātnes padomes (LZP) granti un cits LZP finansējums	46,0
zinātniskās darbības bāzes finansējums	209,1
valsts pētījumu programmu finansējums	48,1
zinātniskās darbības attīstības finansējums	58,3
valsts pārvaldes institūciju pasūtītie pētījumi	
tirgus orientētie pētījumi	10,1
pārējais valsts budžeta finansējums (piemēram, pašvaldību finansējums)	
Augstskolas finansējums zinātnei	0
Finansējums no starptautiskiem avotiem	163,3
tai skaitā ieņēmumi no līgumdarbiem ar ārvalstu juridiskām personām	27,3
Ieņēmumi no līgumdarbiem ar Latvijas Republikas juridiskām personām	5,4

LU Fizikas institūta izpildītie projekti

ES 6. Ietvara Programmas – 5; ES 7. Ietvara Programmas - 3

- *Magnetic flow tomography in technology geophysics and ocean flow research MAGFLOTOM, Commission of the EC, Research DG, Contract No.028670, Specific target Project*
- *Production of a liquid metal limiter for plazma in ISTOK Tokomak, Lisboa, Portugal (production of pumps, flow meters etc.), Fixed contribution contract with EURATOM EC 6 Framework Programm, FU06-CT-2004-00078,*
- *European Isotope Separation On-Line Radiactive Ion Beam facility (EURISOL DS), EC 6 framework Programm, Contract 515768 (RIDS).*
- V*irtual European Lead Laboratory (VELLA), FP6:Contract type: Integrating activities implemented as integrated Infrastructure activities, Project reference 36469. NUWASTE-2005/6-3.2.3.1-1.*
- *The European Spallation Source (ESS),CONSORTIUM AGREEMENT, Latvijas Universitāte (LU**),** LU Fizikas institūts (IPUL)*

2009.gadā apstiprinātie 7.Ietvarprogrammas projekti

- *CP-ESFR Collaboration Project on European Sodium Fast Reactor, no. 232658, 7. ietvarprogramma,*
- *ADRIANA Advanced Reactor Iniative and Network arragement, FP7 RTG,*
- *HeLiMnet . Heavy Liquid Metals Network. Agreement no. 249677*

2008.-2009.g. Līgumi ar ārzemju zinātniskajam institūcijām -9

Zinatniska institūcija	***Valsts***	***Projekta nosaukums***
Paul Scherer Institute	*Šveice*	*Modification o fan electromagnetic pumps*
Corus Research, Development and Technology	*Nīderlande*	*Design, manufacture, test and delivery of a permanent magnet system*
SIEMENS Grenobles Politehniskais institūts CNRS, INPG	*Vācija, Francija*	*Fesible study for the MHD facility with permanent magnets for the glass technology*
SIEMENS Grenobles Politehniskais institūts CNRS, INPG	*Vācija, Francija*	*Manufacturing of prototype*
SCK CEN	*Beļģija*	*Electromagnetic induction pump on permanent magnets*
Los'Alamos National Labarotory (LANL)	*ASV*	*System of electromagnetic pumps*

Oak Ridge National Laboratory (ORNL)	*ASV*	*Design, manufacture, test and delivery 2 electromagnetic pumps*
Forshungszentrum Dresden-Rossendorf(FZD)	*Vācija`*	*Realizations of as Rayleigh-Benard Experiment with mercury in a rotating magnetic field*
Institute for Plasma Research, Gandhinagar, Gujarat	*Indija*	*Design, manufacture of experiemental facilities and conduct eksperiments to study the effects of MHD, corrossion in Pb-Li flow for the development of indian LLCB blanket system*

LU Fizikas institūtā 2008.gadā realizētas 1 valsts pētījumu programmas projekts un 3 sadarbības projekti

Reģistrācijas numurs	***Nosaukums***	***Vadītājs***
Valsts pētījumu programma **„**Modernu funkcionālu materiālu mikroelektronikai, nanoelektronikai, fotonikai, biomedicīnai un konstruktīvo kompozītu, kā arī atbilstošo tehnoloģiju izstrāde” **Rezultāti**	**5. projekts** Nanodaļiņu, nanostrukturālu materiālu un plāno kārtiņu tehnoloģiju izstrāde funkcionālo materiālu un kompozītu izveidei **Apakšapakš projekti:** Modernu funkcionālu mikroelektronikai, nanoelektronikai, fotonikai, bi-omedicīnai un konstruktīvo kompozītu, kā arī to atbilstošo tehnoloģiju izstrāde **Izpildītājs E.Blūms** Nanodaļiņu, nanostrukturālu materiālu un plāno tehnoloģiju izstrāde funkcionālo materiālu un kompozītu izveidei **Izpildītājs A.Cēbers** **1. vadītājs Dr.hab.phys. E.Blūms** Apkopota jaunākā informācija par salikto ferītu nanodaļiņu magnētiskajām īpašībām un izvēlēti magnētiski cietu un magnētiski mīkstu ferītu kompozītu sastāvi eksperimentāliem pētījumiem sadarbības projekta programmas ietvaros. Izmantojot magnetogranulometrijas, magnētiskās dubultlaušanas un gaismas dinamiskās izkliedes mērījumus, izdarīti salīdzinoši pētījumi par dažādu ferokoloīdu nanodaļiņu „magnētisko” un ‘fizisko” izmēru korelāciju. Izstrādāta un aprobēta augstjūtīga un precīza LC oscilatora shēma nanodaļiņu koncentrācijas mērīšanas iekārta ferokoloīdu filtrācijas parādību pētījumiem. Izdarīti nanodaļiņu separācijas dinamikas mērījumi plānā filtrējošā slānī un novērtēts efektīvais termoforēzes koeficients. Izveidots hologrāfiskās inerferometrijas iekārtas makets	E.Blūms E. Cēbers

	un veikti pirmie demonstratīva rakstura eksperimenti koloīdu magnetoforēzes un konvektīvās stabilitātes pētījumiem plānos slānīšos. Veikti skaitliski dubultdifuzīvās magnētiskās konvekcijas stabilitātes pētījumi periodiskās termiski ierosinātās ferokoloīdu satruktūrās un noskaidrotas to likumsakarības. **2. vadītājs Dr.hab.phys. A.Cēbers** 2008 g. Pirmoreiz pasaulē sintezēti lokani feromagnētiski filamenti un eksperimentāli apstiprināta teorētiski paredzētā filamentu anomālā orientācija mainīgā magnētiskā laukā (Publ. : 1.K.Ērglis, M.Belovs, A.Cēbers. Flexible ferromagnetic filaments and the interface with biology. Moscow International Symposium on Magnetism, Book of Abstracts, Moscow , P.238, 2008. 2.K.Ērglis, M.Belovs, A.Cēbers. Flexible ferromagnetic filaments and the interface with biology. Journal of Magnetism and Magnetic Materials – 2009, v.321, P.650-654.) .	
Sadarbības projekti: 1.Nanomateriāli un nanotehnoloģija	a) Mīkstie magnētiskie materiāli un nanotehnoloģijas	A.Cēbers
	b) Difūzā un konvektīvā nanodaļiņu pārneses neizometriskos ferrokoloīdos kapilāri porainās vidēs	E.Blūms
2.06.0029.2.09	MHD metodes dispersās fāzes sadalīšanai un homogenizācijai kompozītos ar metālisku matricu	J.Gelfgats

Institūtā 2009.gadā īstenoti 4 Latvijas Zinātnes padomes finansētie projekti

J.Freibergs 09.1226 ***„Nehomogēna elektromagnētiskā lauka un robežnosacījumu ietekme uz elektrovadošas vides plūsmām"***

Neskatoties uz ierobežoto finansējumu projekts ir veiksmīgi uzsākts. Sasniegti šādi rezultāti:

1. Izgatavoti virkne metamateriāla modeļu elektromagnētisko viļņu kHz un MHz diapazonā. Noteiktas to rezonanses īpašības, ierosinot tiešā, kā arī indukcijas ceļā. Pētot sadarbes īpatnības starp elementiem, konstatēs, ka impulsa ierosmes gadījumā pārmaiņas ierosmes signāli vairākkārt pāriet no viena elementa uz otru. Balstoties uz laboratorijas pētījumiem, modelēti Saules koronas anomālās uzkaršanas mehānismi.
2. Tika izveidota un optimizēta iekārta Pb15.7at%Li sakausējuma ražošanai, kas ļauj iegūt 75 kg sakausējuma vienā sakausēšanas ciklā un veikt vismaz 4 ciklus dienā. Atklātas specifiskās problēmas, kas rodas organizējot sakausēšanas procesu, aprakstīta sakausēšanas iekārtas konstrukcija un tās funkcionēšana procesa laikā. Iegūti tādi termohidrauliskā metālu savienošanās un atdzišanas režīmi, kas ļauj iegūt viendabīgu sakausējumu.
3. V.Kremeņeckis beidza darbu pie fizikas doktora disertācijas un veiksmīgi aizstāvēja to.

2009.gadā veiktie uzdevumi:

Pētīta metamateriālu rezonanses elementu izmantošanu degšanas procesu optimazācijā.

2009.gada pētījumu rezultāti parādīja, ka elektromagnētiskā lauka (EM) kHz un MHz diapazonos var radīt aktīvus metamateriālu elementus ar rezonanses rakstura atbildi uz ārējā lauka iedarbi. Turpmāk paredzēts izpētīt iespēju rezonanses procesus izmantot metamateriālu elementu slodzes gadījumā radot karsēšanas efektus. Iepriekšējie eksperimenti parādīja, ka var elementus izmantot augstas temperatūras degšanas procesu optimizācijā. Iegūtos rezultātus varētu izmantot EM augstfrekvences rezonanses degļa radīšanai, kas varētu rast arī praktisku pielietojumu.

Lai izveidotu droši darbināmu Pb-Li ieguves iekārtu mēģināsim palēināt litija ieplūdes ātrumu un līdz ar to temperatūras kāpumu reaktorā, ja būs atrasts, ka tas nesaasina intermetalītu rašanās problēmu. Tomēr, būtu vēlams reaktorā pārsniegt temperatūru, kurā kūst PbLi - 482 ^{o}C. Veidot reaktoru kompleksā ar elektromagnetisko induktoru un litija inžektoru tādā veidā, lai siltuma izdalīšanās zona koncentrētos reaktora centrā un ar MHD metodēm panākt simetrisku un vienmērīgu siltuma sadalīšanos visā reaktora tilpumā.

A.Gailītis 09.1225

„Šķidrs metāls kodoltehnoloģijās un fizikālos eksperimentos ”

Veiktie darbi:

a) karstā un bezloga variantu salīdzinājums Hg mērķim ekstremāli intensīvā protonu starā (EURISOL parametri):

Fizikas Institūts piedāvā jaunu mērķa konstrukciju, kur protona kūlis (kūļa enerģija 5MW) apstaro šķidro metālu tieši bez starpsienām. Tika izstrādāti vairaki mērķa modeļi, kas mērogā 1:1 ir izmēģināti uz dzīvsudraba kontūra. Eksperimenti parādīja, ka ir iespējams realizēt stabilas šķidra metāla plūsmas ar atbilstošām prasībām – firmas parametri 20 x 600 mm, garums atkarīgs no spiediena caurules kontūra, caurplūde – 12 l/s.

b) daudzstrūklu Ga limitera izpēte Tokamakā ISTTOK un projekta izstrāde limiteram Tokamakā FTU:

Tokamakā ISTTOK (Augstākā Tehniskā skola, Lisabona, Portugāle) veikts limitera uztvertās jaudas mērījumi – parādīts, ka limiters absorbē ap 20% no pilnās izlādes jaudas. Tokamakam FTU (ENEA, Frascati, Itālija) sagatavoti priekšlikumi gallija pievadīšanai – spiedienu ģenerē sistēma ar diviem e.m. sūkņiem, ievadam izmantojot sānu kanālu.

c) sākotnējie eksperimenti ar PbLi kontūru supravadošajā 6 T magnētā

Veikti eksperimentālie pētījumi PlLi kontūrā supravadoša solenoīda magnētiskajā laukā. Eksperimenti pierādīja, ka ar šo iekārtu var veikt ilgstošus korozijas pētījumus pie augstām PlLi temperatūrām (T≤55°C). Pētījumu rezultāti atspoguļoti [3.-5.].

d) parametru definīcija e.m. sūkņiem SNS atskaldīto neitronu avotā:

Veikti aprēķini jaudīgo elektromagnētisko indukcijas sūkņu uz patstāvīgajiem magnētiem smagajiem šķidriem metāliskiem (dzīvsudraba un svina sakausējumiem) parametru novērtēšanai. Izstrādāts jaudīga sūkņa projekts dzīvsudraba spiedienam līdz 5 atmosfērām un caurtecei līdz 10 litriem sekundē. Šāds sūknis kalpo par protipu reālam sūknim ESS apstākļiem.

e) Dinamo-eksperimentu sērija magnētiskās sakabes pārbaudei :

Pārbaude veikta 26-30.04.2009 eksperimentā. Sakabe darbojas teicami un tiks izmantota nākamās eksperimentu sērijās.

E.Blūms 09.1023 **"Liofilizētu magnētisku nanodaļiņu fizikālās īpašības un pārneses parādības stēriski stabilizētos ferrokoloīdos"**

Projekta nelielā finansējuma dēļ ļoti grūti veikt nopietnus eksperimentālos pētījumus, jo nav iespējams iegādāties nepieciešamos materiālus, ķimikālijas un veikt dažādu palīgierīču un mezglu izgatavošanu. 2009. gadā situāciju daļēji glāba papildus finansējums no LZP sadarbības projekta 05.0026. Nanomateriāli un nanotehnoloģijas, (2005.-2009), kura Fizikas institūta apakšprojekts tematiski saistīts ar projektu 09.1023. Pētījumus savstarpēji koordinējot, iegūti šādi kopēji rezultāti:

1. Apkopota jaunākā informācija par salikto ferītu nanodaļiņu magnētiskajām īpašībām un izvēlēti magnētiski cietu un magnētiski mīkstu ferītu kompozītu sastāvi eksperimentāliem pētījumiem projekta programmas ietvaros.
2. Izmantojot magnetogranulometrijas un gaismas dinamiskās izkliedes mērījumus, izdarīti salīdzinoši pētījumi par dažādu ferokoloīdu nanodaļiņu „magnētisko" un 'fizisko" izmēru korelāciju.
3. Izstrādāta un aprobēta augstjūtīga un precīza LC oscilatora shēma (līdz 0.01%) nanodaļiņu koncentrācijas mērīšanas iekārta ferokoloīdu filtrācijas parādību pētījumiem. Izdarīti nanodaļiņu separācijas dinamikas mērījumi plānā filtrējošā slānī un novērtēts efektīvais termoforēzes koeficients.
4. Izveidots hologrāfiskās inerferometrijas iekārtas makets un veikti pirmie demonstratīva rakstura eksperimenti koloīdu magnetoforēzes un konvektīvās stabilitātes pētījumiem plānos slānīšos.

Turpmākie darbi tiks nanodaļiņu pārneses procesu pētījumiem dažādos koloīdos, galveno vērību pievēršot termoforētiskajām, osmotiskām un magnetoforētiskajām parādībām atkarībā no nanodaļiņu izmēra un virsmas īpašībām. Darba konkrētais saturs un pētījumu apjoms atkarīgs no pieejamā finansējuma.
finansējumam, kas ļautu uzlabot konkrētus tehnoloģiskos procesus , pielietojot elektromagnētiskā lauka iedarbi.

I.Grants 09.1223 **Elektromagnētisko lauku ietekme uz kustības, siltuma un masas pārneses procesiem elektrovadošas vides virpuļplūsmās**

Ir izveidota eksperimentālā iekārta, lai izvērtētu nehomogēna magnētiskā lauka ietekmi uz degšanas procesu dinamiku liesmas virpuļplūsmā. Ir veikti degšanas procesu dinamikas pētījumi liesmas virpuļplūsmā, kas ietver kompleksus liesmas ātruma, temperatūras un sastāva sadalījuma veidošanās pētījumus dažādās atjaunojamā kurināmā (koksnes biomasas) degšanas procesa attīstības stadijās, izvērtējot nehomogēna magnētiskā lauka ietekmi uz degšanas un siltuma/ masas pārneses procesiemprocesiem. Pētījumu rezultāti ir aprobēti Starptautiskā BIO NORD Konferencē un 50. RTU Starptautiskā Zinātniskā Konferencē Rīgā. Ir sagatavotas un iesniegtas publikācijas žurnāliem „Global Nest" (citējams izdevums) un LFTZ.

Pārskata periodā uzprojektēta eksperimentālā iekārta koncentrētā virpuļa un tā izraisītās šķidra metāla virsmas deformācijas novērošanai. Šī iekārta izgatavota sadarbībā ar *Forschungszentrum Dresden-Rossendorf*, kur arī veikti eksperimenti ar to. Iegūtie rezultāti apstiprināja izvirzīto hipotēzi, ka magnētiskie tilpuma spēki var ierosināt koncentrētu virpuli noslēgtā tilpumā. Parādīts, ka ierosinātajam virpulim

ir vairākas līdzības ar atmosfēras virpuļiem: rotējošās plūsmas maksimālo ātrumu nosaka poloidālais spēks tāpat kā orkāna vēja ātrumu nosaka spiediena deficīts tā centrā., bet azimutālais spēks nosaka virpuļa struktūru. Parādīts, ka azimutālajam tilpuma spēkam piemīt sviras daba. Proti, būdams daudzkārt mazāks par primāro poloidālo, tas būtiski izmaina ātruma sadalījumu. Iegūtie rezultāti arī parādīja, ka turbulence ierobežo minimālo virpuļa diametru, kā rezultātā virsmas deformācija ir telpiski izplūdusi un nepastāvīga. Tādejādi, iegūtā plūsma nav noderīga peldošu daļiņu ātrai iemaisīšanai tilpumā, kas ir pētāmās parādības galvenais praktiskais pielietojums. Plānotie darba mērķi šajā pētījumu virzienā ir pilnībā sasniegti neskatoties uz finansējuma trūkumu, kura dēļ eksperiments tika veikts pie sadarbības partneriem Drēzdenē. Turpmāko pētījumu uzdevums ir atrast veidus kā stabilizēt virpuli, panākot, ka uz metāla virsmas veidojas izteikta piltuve ar lejup vērstu virsmas ātrumu. Iespējamie risinājumi ir stabilizācija ar inerci virpuļa iegriešanās laikā kā arī stabilizācija ar pastāvīgu aksiālu magnētisko lauku. Pētījumus paredzēts tupināt kā ar eksperimentālām, kā arī skaitliskām metodēm.

Grants I. 05.1465 ***Nestabilitātes un pāreja uz turbulenci elektrovadošo šķidrumu plūsmās ārējos magnētiskajos laukos***

Izpētīti nosacījumi skrejoša magnētiskā lauka parametriem, kas nepieciešami, lai izmainītu kausējuma plūsmas virzienu virs ieliktas sacietēšanas frontes VGF (*Vertical gradient freeze*) kristālu audzēšanas procesos. Šāda ietekme lietderīga piemaisījumu radiālās segregācijas samazināšanai neliela izmēra pusvadītāju monokristālu ražošanā. Pētījumi aptver plašu vadošo parametru intervālu, kas ļauj pielietot rezultātus dažādiem procesiem. Atklāts, ka dabiskā konvekcija ierosina automodulāru robežslāņa tipa plūsmu virs kristalizācijas frontes ar netriviālu atkarību no Grashofa un Prandtļa skaitļiem. Neskatotoies uz to, nepieciešamā skrejošā lauka intensitāte dabiskās plūsmas pagriešanai pretējā virzienā ir proporcionāla vienkārši Grashofa skaitļa un frontes ieliekuma dziļuma reizinājumam. Pētījumu rezultāti publicēti žurnālā *Journal of Crystal Growth*.

Turpinot augstākminētos pētījumus veikta skrejošā magnētiskā lauka ierosinātas plūsmas skaitliska stabilitātes analīze kristālaudzēšanas procesos ar VGF metodi. Noskaidrots, ka gadījumā, ja lauks tiek izmantots radiālās piemaisījumu segregācijas samazināšanai, tad plūsma praktiski vienmēr paliek stabila. Skrejošais lauks var tikt izmantots arī cita mērķa sasniegšanai – kristalizācijas frontes ieliekuma samazināšanai. Šim nolūkam pielietojams lejup vērsts skrejošais magnētiskais lauks. Noskaidrots, ka izteikts šāda veida efekts ir savienojams ar plūsmas stabilitāti, ja audzējamā kristāla radiuss pārsniedz noteiktu lielumu. VGF procesam raksturīga stabila kausējuma vertikālā stratifikācija. Šāds temperatūras gradients ievērojami bremzē un stabilizē plūsmu. Stabilitātes analīze veikta plašam vadošo parametru intervālam. Novērotas vairākas interesantas parādības – zemkritiskā nestabilitāte, "stabilitātes salu" veidošanās. Skaitlisko pētījumu rezultāti daļēji pārbaudīti eksperimentā. Pētījumu rezultāti sagatavoti publikācijai žurnālā *Journal of Crystal Growth*.

Projekta pieteikumā plānotie darba uzdevumi pamatā ir izpildīti. Papildus projekta iesniegumā paredzētajam, veikti eksperimenti ar magnētisko tilpumspēku ierosinātu virpuļplūsmu šķidra metāla cilindrā. Pētījumu mērķis bija noskaidrot nosacījumus, pie kādiem veidojas intensīvs koncentrēts virpulis, kā arī šāda virpuļa raksturīgās īpašības. Eksperimentā novēroti trīs režīmi: (1) koncentrēts virpulis; (2) iekšēja kodola veidošanās; (3) meridionālās plūsmas apspiešana. Pirmajos divos režīmos novērotas vairākas līdzības ar atmosfēras virpuļiem: (1) virpuļa intensitāti nosaka

meridionālās plūsmas avota intensitāte; (2) virpuļa struktūru nosaka leņķiskā momenta un meridionālās plūsmas avotu attiecība; (3) Plūsmas iekšējā kodolā meridionālā plūsma maina virzienu līdzīgi kā orkāna "acī". Magnētisko spēku izmantošana būtiski papildina iepriekš izmantotos atmosfēras virpuļu modeļus ar to, ka šie spēki principā ir neatkarīgi no plūsmas. Turklāt, divu savstarpēji neatkarīgu magnētisko spēku izmantošana ļauj samērot abas virpuļa pastāvēšanai nepieciešamās komponentes – meridionālo un azimutālo. Eksprimentā parādīts, ka azimutālam spēkam ir sviras daba – salīdzinoši ļoti vājš azimutāls spēks var būtiski izmainīt virpuļa struktūru. Pētījumu rezultāti publicēti žurnālā *Journal of Fluid Mechanics*.

2009. gada raksti starptautiski citētos izdevumos - 23

1. I.Grants, A.Klyukin, G.Gerbeth (2009) *Instability of the melt flow in VGF growth with a traveling magnetic field J.Crystal Growth* ,**311**, 4255
2. A.Cramer, V.Galindo, G.Gerbeth, J.Priede, A.Bojarevics, Yu.Gelfgat, O.Andersen, C.Kostmann. T*ailored Magnetic Fields in the Melt Extraction of Metallic Filaments.* METALLURGICAL AND MATERIALS TRANSACTIONS B, 2009, vol.40B, p.337-344.
3. R. B. Gomes, H. Fernandes, C. Silva, A. Sarakovskis, T. Pereira, J. Figueiredo, B. Carvalho, A. Soares, P. Duarte, C. Varandas, O. Lielausis, A. Klyukin, E. Platacis, I. Tale, A. Alekseyv. *Liquid gallium jet-plasma interaction studies in ISTTOK tokamak*. Journal of Nuclear Materials 390-391 (2009) pp. 938-941
4. 3.3. Rade Ž. Milenkovic, S. Dementjev, K.Samec, E.Platacis, A.Zik, A.Flerov, Kn.Thomsen. *Structural-hydraulic test of the liquid metal EURISOL target mock-up.* Journal Nuclear Instruments an Methods in Physics Research, Article in press.
5. R. Krishbergs, E. Ligere, F. Muktepavela, E. Platacis, A. Shishko, A. Zik. *Eksperimental studies of the strong Magnetic field action on the corrosion of RAFM Steels in Pb17Li melt flows.* Magnetohydrodinamics Vol.45(2009), Nr. 2., pp. 289-296
6. Cyril Kharoua, Yacine Kadi, Erik Platacis, Kalvis Kravalis and the EURISOL-DS Task#2 collaboration. EURISOL-DS Multi –MW Target Study of the Windowless Transverse Film Liquid Metal Proton-to-Neutron Converter. CERN-EN-NOTE-2009-003 STI.
7. D. Zablotsky, V. Frishfelds, E. Blums. Investigation of heat transfer efficiency of thermomagnetic convection in ferrofluids, *Magnetohydrodynamics*, 2009, vol. **45**(3), pp. 267–271.
8. D. Zablotsky, A. Mezulis, E. Blums. Surface cooling based on the thermomagnetic convection: Numerical simulation and experiment. *Int. J. Heat Mass Transfer.*, 2009, vol. **52**, pp. 5302-5308.
9. Zablotskaya, I. Segal, E. Lukevics, M. Maiorov, D.Zablotsky, E. Blums, I. Shestakova, I. Domracheva. Water-Soluble Magnetic Nanoparticles With Biologically Active Stabilizers, *JMMM*, **321** (2009), 1428-1432, Doi Information: 10.1016/J.Jmmm. 2009.02.060.
10. M. Zaķe, I. Barmina, A. Descnickis, V. Krishko, M. Gedrovics, Experimental study of the combustion dynamics of renewable&fossil fuel co-fire in swirling flame, In: Latvian Journal of Physics and Technical Sciences, 2009, Vol 46, Nr.6, pp 3-16.
11. E.Karule, A.Gailitis. Above threshold ionization of atomic hydrogen in *ns* states with up to four excess photons. J.Phys. B: At. Mol. Opt. Phys. **43** (2010) 065601 (7 lpp)

12. V. Bojarevics and K. Pericleous. “Droplet oscillations in high gradient static magnetic field”. Microgravity Science and Technology, 2009, vol. 21, N 1-2, pp. 119-122. ISSN 0938-0108 (Print), 1875-0494 (Online). DOI: 10.1007/s12217-008-9055-y
13. V. Bojarevics and K. Pericleous. “Dynamic melting model for small samples in cold crucible”. The International Journal for Computation and Mathematics in Electrical and Electronic Engineering, 2008, vol 27, No. 2, pp. 350-358. **DOI:** 10.1108/03321640810847634, ISSN 0332-1649, ISBN 978-1-84663-764-3
14. V. Bojarevics, K. Pericleous and R. Brooks. “Dynamic Model for Metal Cleanness Evaluation by Melting in Cold Crucible”, Metallurgical and Materials Transactions, B, 2009, v. 40, N 3, pp. 328 – 336. ISSN 1073-5615, DOI: 10.1007/s11663-009-9226-2
15. G. Djambazov, V. Bojarevics and K. Pericleous. “Vacuum Arc Remelting Time dependent Modelling”. Magnetohydrodynamics, 2009, Vol. 45, No. 4, pp. 475–482.
16. V. Bojarevics, K. Pericleous. “Levitated droplet oscillations: effect of internal flow. Magnetohydrodynamics”, 2009,Vol. 45, No. 3, pp. 267–276.
17. P.Tierno, J.Claret, Fr.Sagues, and A.Cēbers. Overdamped dynamics of paramagnetic ellipsoids in a precessing magnetic field. Phys.Rev.E- 2009, v.79, 021501
18. K.Ērglis, M.Belovs, A.Cēbers. Flexible ferromagnetic filaments and the interface with biology. Journal of Magnetism and Magnetic Materials – 2009, v.321, P.650-654.
19. M.Belovs, A.Cēbers. Properties of twisted ferromagnetic filaments. Journal of Physics:Conf.Ser. -2009, v.149, 012103.
20. E.Wandersman,E.Dubois,F.Cousin,V.Dupuis,G.Meriquet,R.Perzynski, and A.Cēbers. Relaxation of the field-induced structural anisotropy in a rotating magnetic field. Europhysics Letters – 2009,v.86,10005.
21. M.Belovs, and A.Cēbers. Ferromagnetic microswimmer. Phys.Rev.E – 2009, v.79, 051503;Erratum:Ferromagnetic microswimmer [Phys.Rev.E 79,051503 (2009)]. Phys.Rev.E – 2009, v.79, 069906(E).
22. M.Belovs, T.Cīrulis, and A.Cēbers. Equilibrium shapes of twisted magnetic filaments. J.Phys.A:Math.Theor. – 2009,v.42, 235206
23. C.Gourdon,V.Jeudy, A.Cēbers, A.Dourlat, Kh.Khazen, and A.Lemaitre. Unusual domain-wall motion in ferromagnetic semiconductor films with tetragonal anisotropy. Phys.Rev. B – 2009, v.80, 161202(R).

2009. gada raksti Starptautisko konferenču rakstu krājumos (Proceeding) -25

I Proceedings of 6th Intl. Conf. on Electromagnetic Processing of Materials, Dresden (EPM 2009), ISBN 978-3-936104-65-3

1. I.Grants, A.Klyukin, G.Gerbeth (2009) *Flow stability in magnetically manipulated vertical gradient freeze,*
2. I.Grants, G.Gerbeth (2009) *Liquid metal tornado,*
3. A. Pedchenko, A. Bojarevics, J. Priede, G. Gerbeth, R. Hermann. Model experiments on the melt flow driven by a two-phase inductor.
4. Rade Ž. Milenkovič, Sergejs Dementjevs, Karel Samec, Ernests Platacis, Anatolij Zik, Aleksej Flerov, Knud Thomsen, Enzo Manfrin. *Time-frequency analysis of coupled structural-hydraulic behavior of the EURISOL liquid metal target mock-up*. pp. 425-428
5. K. Kravalis, F. Muktepavela, E. Platacis, A.Shishko. *Experimental Results on the Magnetic Field Influence on the Corrosion of EUROFER Steel in Pb17Li Flow*. pp. 473-475

6. Valdmanis, A. Cipijs. *"High Frequency Electromagnetic Resonant Heating Effects. lpp. 149-153.*
7. J.E.Freibergs, I.Platnieks, *Magnetohydrodynamic technology for lead-lithium alloy production. Proceedings. pp.834-837.*
8. V. Bojarevics and K. Pericleous. "Solutions for the metal-bath interface in aluminium electrolysis cells", Light Metals 2009, Ed. G. Bearne, TMS, 2009, p. 569-574. ISBN Number 978-0-87339-731-5, ISSN Number 109-9586.
9. V.Bojarevics, S.Easter, A.Roy, K.Pericleous. Magnetic Damping of Levitated Liquid Droplets in AC and DC Field. Proceedings 6th Int. Conf. Electromagnetic Processing of Materials (**keynote lecture)**, 2009, Dresden, pp. 699-702. ISBN 978-3-936104-65-3
10. V.Bojarevics. Models for magnetohydrodynamics of aluminium electrolysis cells. Proceedings 6th Int. Conf. Electromagnetic Processing of Materials, 2009, Dresden, pp. 90-93. ISBN 978-3-936104-65-3
11. S.Easter, V.Bojarevics, K.Pericleous. Determining Surface Tension Using DC Magnetic Levitation. Proceedings 6th Int. Conf. Electromagnetic Processing of Materials, 2009, Dresden, pp. 723-726. ISBN 978-3-936104-65-3
12. S.Taniguchi, S.Shimasaki, J.S.Park, K.Ueno, V.Bojarevics. Prospect for EPM Application to Environmental Technology. Proceedings 6th Int. Conf. Electromagnetic Processing of Materials, 2009, Dresden, (**plenary lecture),** pp. 3-8. ISBN 978-3-936104-65-3
13. S.Shimasaki, K.Imanishi, S.Taniguchi, V.Bojarevics. Manufacturing of Uniformly Shaped Silicon Particles for Solar Cell from Molten Metal Jet by Electromagnetic Pinch Force. Proceedings 6th Int. Conf. Electromagnetic Processing of Materials, 2009, Dresden, pp. 899-902. ISBN 978-3-936104-65-3
14. V. Bojarevics and K. Pericleous. "Solutions for the metal-bath interface in aluminium electrolysis cells", Light Metals 2009, Ed. G. Bearne, TMS, 2009, p. 569-574. ISBN Number 978-0-87339-731-5, ISSN Number 109-9586.

II Proceedings International Symposium on Liquid Metal Processing and Casting, 2009, Santa Fe

15. V. Bojarevics, S. Easter, K. Pericleous. Levitated Liquid Droplets in AC and DC Magnetic Field., pp. 319-326. ISBN 978-0-87339-743-8

III Proceedings of 2nd Nordic Wood Biorefinery Conference (NWBC 2009), Helsinki, Finland, 2009,

1. G. Telysheva, A. Arshanitsa, T. Dizhbite, A. Andersone, G. Lebedeva, I. Barmina, M. Zake, *Multiple Products on the Basis of Rich-in-Lignin Residues from Bio-Ethanol Production – an Approach to Realization of the Biorefinery Concept*, 9, pp.80-88.

IV International Conference on Peaceful Uses of Atomic Energy-2009
***Vigyan Bhavan, New Delhi, India, SE-6-2*, September 29 – October 1, 2009**

1. E. Platacis. *Liquid metal research activities at Institute of Physics University of Latvia*
2. J.E. Freibergs. *Industrial Production Technology of Lead-Lithium Alloy., pp.66-67.*

V ICANS XIX, 19th meeting on Collaboration of Advanced Neutron Sources, March 8-12, 2010 Grinderwald, Switzerland.

1. K. Thomsen, K. Conder, Y. Dai, D. Kiselev, M. Medarde, R. Moormann, J. Neuhausen, E. Platacis, E. Pomjakushina, S. Torok, L. Zanini, P. Zimmermann. *Lead Gold Eutectic, First Steps Towards the Qualification of a Novel Target Material for ESS*

VI EURISOL conference, Pisa, 3.03.09 Starptautiskā plazmas konferencē EJC-PISE-2009

.K.Kravalis, E. Platacis, A. Ziks, J. Kadi, C. Kharona. *Towards Transverse Windowless Target*.

VII 3-th Congress on Advenced Electromagnetic Materials in Microwaves and Optics Metamaterials 2009. London 2009 (CD).

J. Valdmanis, A. Cipijs.*"Investigation of resonant metamaterials elements for MHz frequency". 3-th Congress on Advenced Electromagnetic Materials in Microwaves and Optics. Metamaterials 2009. London 2009 (CD).*

VIII 19th PSI conference , San Diego

R. B. Gomes[1], H. Fernandes[1], C. Silva[1], P. Duarte[1], O. Lielausis[2], A. Klyukin[2], E. Platacis[2] and A. Alekseyv[3] , *[1]Associação EURATOM/IST, Instituto de Plasmas e Fusão Nuclear/IST, Av. Rovisco Pais, No. 1, 1049-001 Lisboa, Portugal.*

[2]Association EURATOM/University of Latvia, [3]TRINITI Troitsk, Moscow reg. 142190, Russia. Dynamic behaviour of a Liquid Gallium Jet under the Influence of the Tokamak ISTTOK Plasmas

IX Joint European Thermodynamics Conference JRTC-10, 22. June – 24. June 2009, Kopenhagen, Danmark

Blums E., Kronkalns G., Mezulis A., Sints V. Thermoosmotic transfer of ferrocollo-ids through a capillary porous layer in the presence of uniform magnetic field, http://www.jetc10.fys.ku.dk/?q=allabstracts.

X International seminar in Tallin June 11-14, 2009. Radiation Fields of Erath, related Architectural Geometry of Forms and their Influence on Organisms.

J.Valdmanis, A.Cipijs, J. Dolacis. *Dowsing as resonant interaction*, Proceeding – Abstracts and Articles, page 40-43

XI APS March Meeting, Pittsburgh

A.Cēbers, M.Belovs, K.Ērglis. Flexible ferromagnetic filaments and the interface with biology., W15_7, P.493, 2009.

Training school on magneto sciences (Riga, Latvia, May 18 – 22, 2009) supported by COST P17) with the participation of teachers from the European group of teachers GAMAS - 5

1. Elmars Blums. Heat and mass transfer in magnetic nanocolloids, Proceedings, Vol. **2**, p.180 – 202.
2. A.Gailitis, *Laboratory experiments on MHD DYNAMO.* Proceedings, Vol. **2**.
3. J.Freibergs .*Electrolysis cells of aluminium.* Proceedings, Vol. **2**.
4. Y.Gelfgat *Electromagnetic methods and devices for melting, transportation, stirring and preparation of Al.-alloys.* Proceedings, Vol. **2**.
5. A. Cebers. Soft *magnetic micro machines* Proceedings, Vol. **2**, P.150-179.

Ziņojumi - 2

1. J.Freibergs no 25.03.2009 līdz 29.03.2009 piedalījās seminārā „*Future Prospectives in Magnetosciences, Applications to Energy and Materials"* Grenoblē, Francijā, SIMAP ar referātu "Liquid Metal MHD Experiments at IPUL".
2. J.Freibergs 16.06.2009 piedalījās *7IP projekta CP ESFR SP4* konsultatīvajā sapulcē, Lionā, Francijā, AREVA un nolasīja referātu „EMP pielietojumu iespējām nātrija dzesētos ātrajos reaktoros", aut. J.Freibergs, I.Bucenieks, A.Pozņaks.

Starptautiskās konferences Latvijā-11

1. E. Platacis. A. Šiško, F. Muktepāvela, R. Krišbergs. *Ekspluatācijas faktoru (T,t,B) ietekmes izpēte uz blanketa EUROFER tērauda korozijas procesiem Pb-Li plūsmā*. LUCFI 25. Zinātniskās konfrences tēzes. 2009, 11-13. februāris. P 70.
2. V.Kremeņeckis piedalījās *„Rīgas Tehniskās Universitātes 50. starptautiskā zinātniskā konferencē"* ar referātu: „Precīzie automodulārie atrisinājumi hidrodinamikā un magnētiskajā hidrodinamikā un to attiecība pret uzdevumiem robežslāņa tuvinājumā." Rīga, 2009. gada 12. – 16. oktobrī.
3. I. Barmina, M. Gedrovics, V. Krishko, M. Zake , Co-firing of the renewable with fossil fuel for the clean and effective heat energy production, VIII International Conference BIONORM II, RTU "Environmental and climate technologies" ser.13, N2, pp. 21-30, 2009, Riga**.**
4. A. Arshanitsa, I. Barmina, G. Telysheva, T. Dizhbite, A. Andersone, M. Zake, I. Grants, *The composition and fuel characteristics of non-hydrolyzed residues from wheat straw ethanol production,* IX 8th International Scientific Conference "Engineering for Rural Development"*In: "Engineering for Rural Development", Jelgava, 2009, pp. 105-111.*
5. I**.** Barmina, I. Bucenieks, M. Gerdovičs, V.Kriško, M. Zake, *The magnetic field effect on the swirling combustion of the renewable fuel,* 50th International Scientific Conference *In: Environmental and Climate Technologies, ser.13, Nr.3; Riga, RTU, 2009, pp.11-19.*

International conference „Functional materials and nanotechnologies FM&NT-2009, Riga, March 31 – April 3, 2009

1. D. Zablockis, V. Frishfelds, E. Blums. Numerical investigation of thermomagnetic intensification of heat transfer in ferrofluids,

2. M. Maiorov, G. Kronkalns, E. Blums. Ferrite nanoparticles under the effect of low-frequency magnetic field.

3. A. Mežulis, Measuring the transport coefficients of nanoparticles by a continuous power laser,

4. A. Zablotskaya, I. Segal, A. Svarinsky, T. Eremkina, M. Maiorov, I. Dolmachova, Synthesis, physico-chemical study and cytotoxic properties of magnetite nanoparticles bearing silyl(n,n-dimethil)ethanolamines,

5. I. Segal, A. Zablotskaya, K. Savicka, M. Maiorov, D. Zablocky, I. Shestakova, Water soluble ireon oxide/oleic acid magnetic nanoparticles: preparation, physico-chemical and biological characteristics

F**irst International EJC-PISE Workshop in Riga**

J.Valdmanis, A.Cipijs. *High frequency electromagnetivc resonant method for metals melting and vaporization.*

Reģistrētie patenti:

2 patenti

LV patents	I. Barmina, M.Gedrovičs, P. Meija, A. Meijere-Līckrastiņa, M. Purmals, M. Zaķe, Atjaunojamā kurināmā un gāzveida kurināmā vienlaicīgas sadedzināšanas apkures katls-LV patenta pieteikums P-08-20,ekspertīzes lēmums 2/1307, 20.09.2009., pp.1-16.
European Patent	(Application No.08016830.5-2209) "Vervahren und Anordnung zur Messung des Durchflusses elektrisch leitfahiger medien" (2008). Autori: G.Gerbeth, … A.Bojarevics, … J.Gelfgats.

Institūta (augstskolas) 2008.gadā īstenoto tirgus orientēto pētījumu vai pašvaldību pasūtījumu skaits un nosaukums: 1 līgums

IZM TOP08-17	Titāna ražošanas tehnoloģijas izstrādāšana, bāzējoties uz savstarpēju titāna tetrahlorida un metāliskā magnija tvaiku savstarpēju mijiedarbību"	E.Platacis

Promocijas darbs - 1:

- **V.Kremeņeckis 2009. gada 26. jūnijā sekmīgi aizstāvēja promocijas darbu fizikas doktora grāda iegūšanai. Promocijas darba nosaukums: „Precīzie automodulārie atrisinājumi hidrodinamikā un magnētiskajā hidrodinamikā un to attiecība pret uzdevumiem robežslāņa tuvinājumā." Darba vadītājs J.Freibergs.**

Maģistra darbi – 2

- **Imanta Kaldres** aizstāvētais maģistra darbs - **Termoelektrisko strāvu un magnētiskā lauka mijiedarbības izraisītas šķidra metāla plūsmas eksperimentāla izpēte adatveida režģa apkārtnē.** Experimental study of liquid metal flow, created by thermoelectric currents and magnetic field interaction, around needle array.

- Maija Zaķe – piedalījās V. .Kriško **maģistrantūras darba „**Atjaunojamo energoresursu un gāzveida fosilā kurināmā līdzsadedzināšana videi draudzīgākai enerģijas ražošanai**" vadīšanā, kuru V.Kriško aiztāvēja 2009.gada jūnijā. No 2010. gada jūlija - RTU doktorantūra**

- **Bakalaura darbu aizstāvēja un iestājās maģistranturā - Toms Beinerts**

LU Fizikas institūta doktoranti – 6

K.Kravalis – vadītājs dr.fiz. Imants Bucenieks
G.Lipsbergs – vadītājs dr.fiz. Agris Gailītis
D.Zablockis - vadītājs dr.hab.fiz. Elmārs Blūms
I.Kaldre – vadītājs LU FI A.Bojarēvičs
A.Desņickis – vadītāji: dr.fiz. Maija Zaķe (LUFI) un Dr. Sci. ing. Mārtiņš Gedrovičs (RTU)
V Krishko – vadītāji: dr.fiz. Maija Zaķe (LUFI) un Dr. Sci. ing. Mārtiņš Gedrovičs RTU

LU Fizikas institūta magistrants

Toms Beinerts, vadītajs Andris Bojarēvičs

Lekciju kurss MHD - LU Fizikas un matemātikas fakultātes studentiem – sagatavojis un lasījis A.Gailītis

Jaunie zinātnieki - 6

1. Ansis Mežulis, aizstāvēja promocijas darbu 2000.g.
2. Inesa Barmina, aizstāvēja promocijas darbu 2003.g.
3. Aleksandrs Pedčenko promocijas darbu aizstāvēja 2004.g.
4. Armands Krauze aizstāvēja promocijas darbu 2005.g.
5. Agnese Līckrastiņa (Meijere) - LUFI vadošā pētniece, Dr. sc. ing., statuss-jaunā zinātniece (promocijas darbs "Wood biomass(granules) co-firing with gaseous fuel (propane)", kuru aizstāvēja 2005. gada aprīlī.
6. V.Kremeņeckis 2009. gada 26. jūnijā sekmīgi aizstāvēja promocijas darbu fizikas doktora grāda iegūšanai. Disertācijas nosaukums: „Precīzie automodulārie atrisinājumi hidrodinamikā un magnētiskajā hidrodinamikā un to attiecība pret uzdevumiem robežslāņa tuvinājumā." Darba vadītājs J.Freibergs.

Studenti - 5
LU students I.Šints, darbus vada A.Mežulis
LU studenti L.Magones, I.Magones-Jaunpetroviča darbu vada A.Gailītis
RTU studentu I.Pagasta, G.Mencendorfa un L.Goldšteina darbu vada Dr.Platacis

University of Latvia Institute of Physics

ELECTROMAGNETIC PROCESSING DURING PRODUCTION OF METAL-MATRIX COMPOSITES

Andris Bojarevičs, Jurijs Gelfgats,
Imants Bucenieks, Toms Beinerts

Tel. 29506985
e-mail: andrisb@sal.lv

INSTITUTE OF PHYSICS, UNIVERSITY OF LATVIA
lab of MHD-technologies

FIELD OF EXPERTISE

- Liquid metal flow controlled by Electromagnetic field
- Electromagnetic pumps, stirrers, throttles, instability damping etc. ….

Recent projects for industry:

- Siemens-VAI
- Corus in alliance with POSCO
- Schott AG
- Wacker (Siltronic AG)

2

Potential Products

- Electromagnetic Processing Equipment for Modern Metallurgy
- Production lines for **Metal-Matrix-Composites (MMC)**

3

Aluminium World Consumption

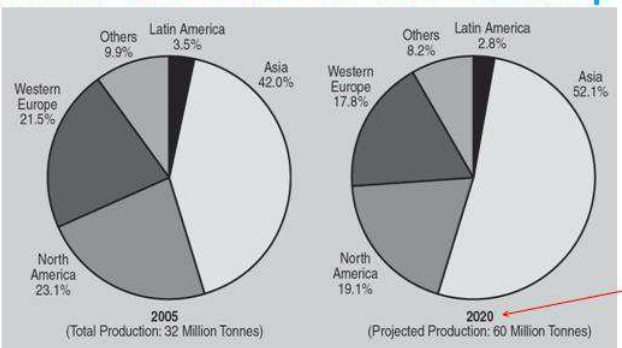

$ 120*10^9

Figure 1. The world consumption of primary aluminum, in millions of tonnes.[1,4,10]

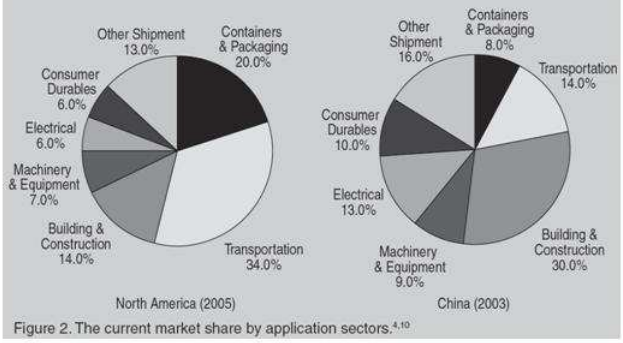

Figure 2. The current market share by application sectors.[4,10]

4

Light and small product replaces the traditional

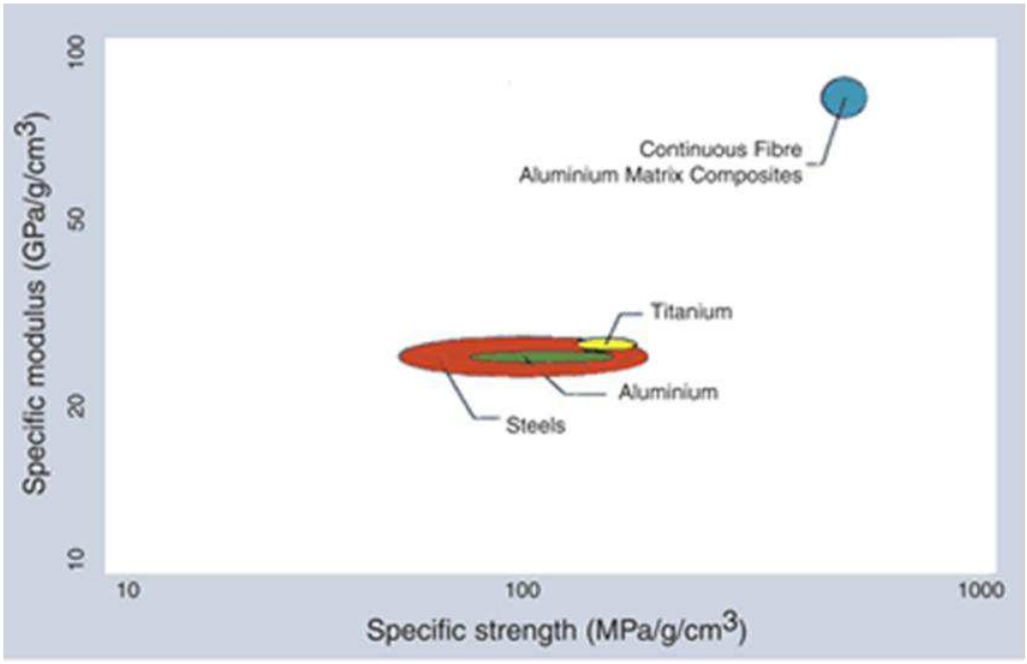

5

Where to invest?

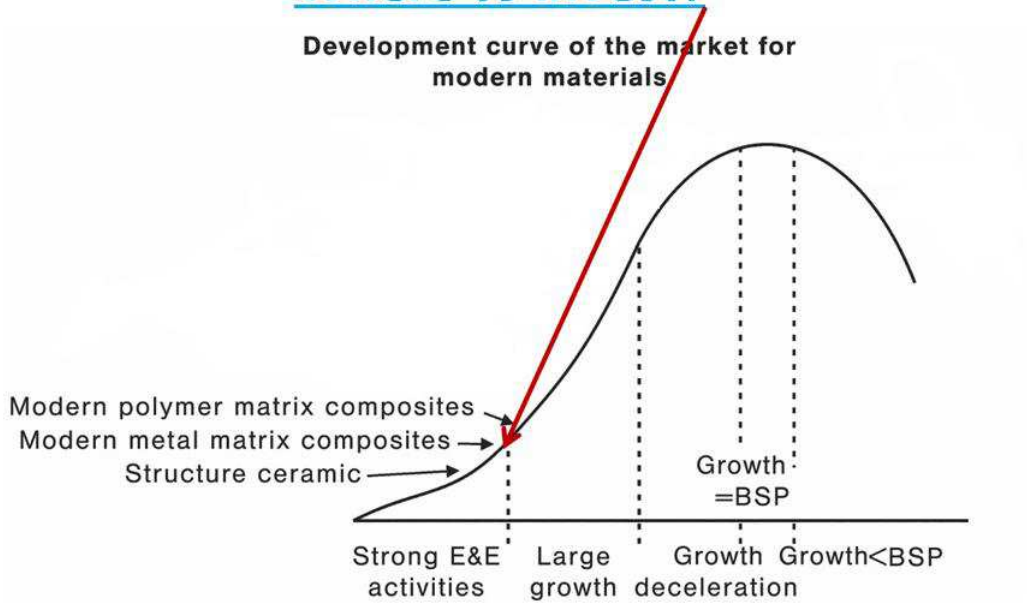

6

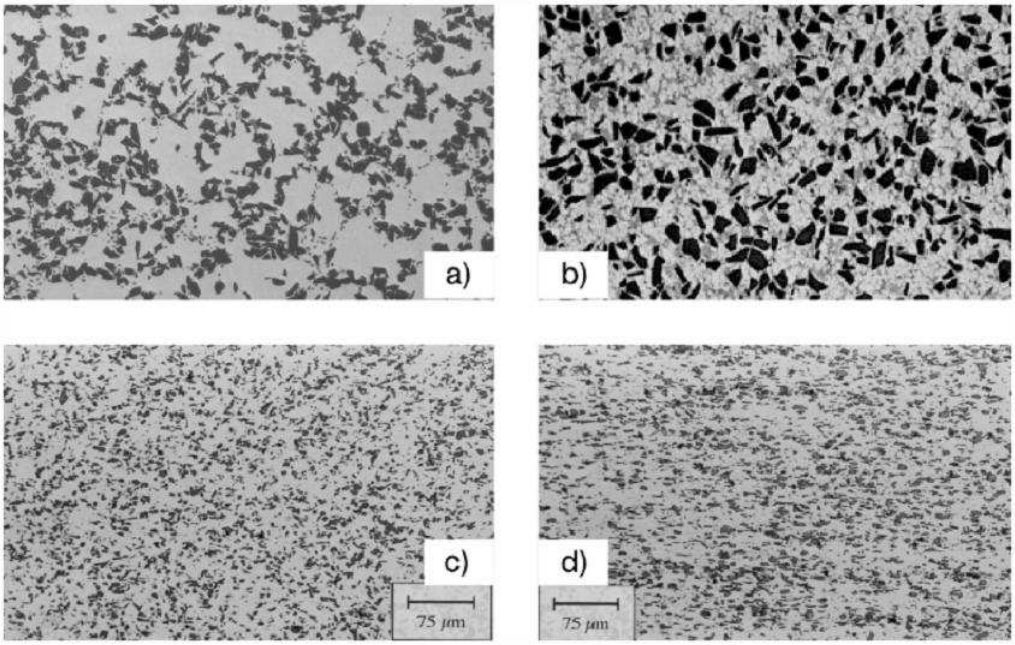

Fig. 1.57 Arrangement of typical structures of different particle reinforced light metal composite materials: (a) SiC-particle reinforced Al (mold cast [9]), (b) SiC-particle reinforced Al (die cast [10]), (c) SiC-particle reinforced Al (extruded powder mixture [11]), (d) SiC- particle reinforced Al (cast and extruded).

7

Applications of MMC

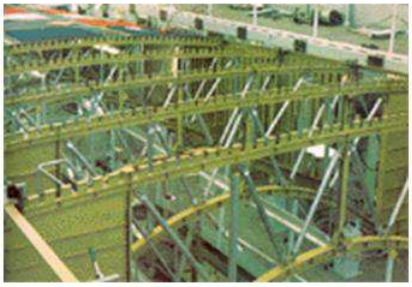

Figure 1. Mid-fuselage structure of Space Shuttle Orbiter showing boron-aluminum tubes. (Photo courtesy of U.S. Air Force/NASA).

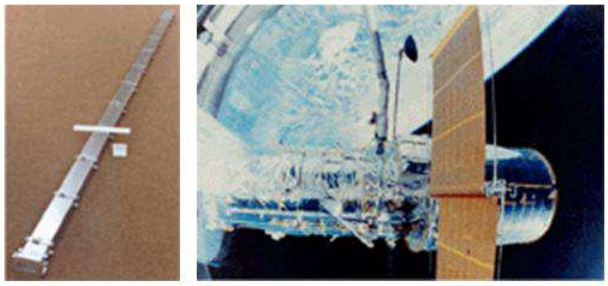

Figure 2. The P100/6061 Al high-gain antenna wave guides/ boom for the Hubble Space Telescope (HST) shown (a-left) before integration in the HST, and (b-right) on the HST as it is deployed in low-earth orbit

8

Basics of Metal Matrix Composites

Karl Ulrich Kainer

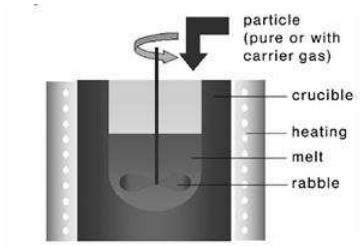

Fig. 1.7 Schematic operational sequence during melt stirring.

In general, the **major advantages** of Aluminium Matrix Composites (AMCs) compared to unreinforced materials, such as steel and other common metals, are as follows:

Increased specific strength
Increased specific stiffness
Increased elevated temperature strength
Improved wear resistance
Lower density
Improved damping capabilities
Tailorable thermal expansion coefficients
Good corrosion resistance

9

Figure 4. Cast SiC_p/Al attachment fittings: (a-top) multi-inlet fitting for a truss node, and (b-bottom) cast fitting brazed to a Gr/Al tube.

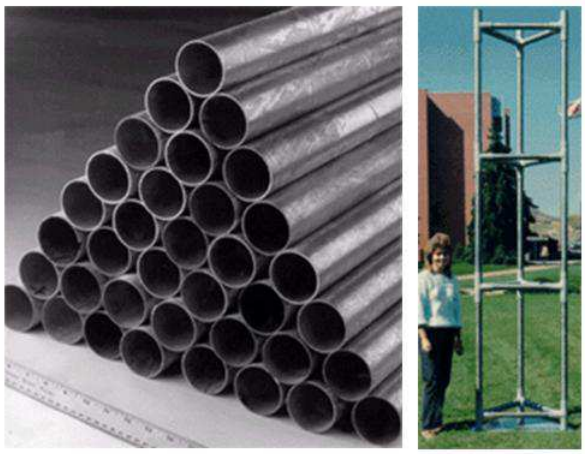

Figure 4. Cast SiC_p/Al attachment fittings: (a-top) multi-inlet fitting for a truss node, and (b-bottom) cast fitting brazed to a Gr/Al tube.

10

Model of a mixer for Aluminium furnaces
to produce uniform Metal-Reinforcement mixture in a large volume

11

Funnel-type flow of liquid metal

Electromagnetic Method and Device for Mixing up Fine Scrap and Alloying Additions into Molten Metal
Institute of Physics, University of Latvia

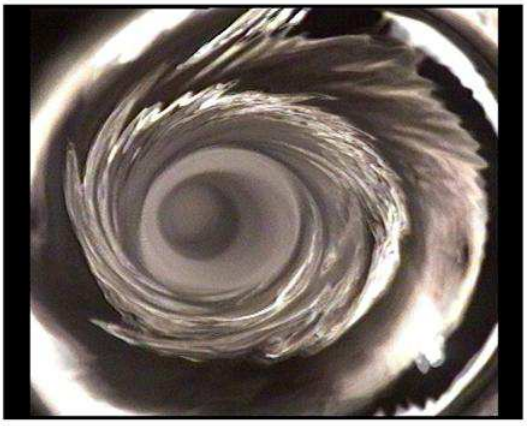

Photo of the EMF when operated in mode 2.

12

Electromagnetic Method and Device for Mixing up Fine Scrap and Alloying Additions into Molten Metal
Institute of Physics, University of Latvia

Schematic Presentation of the Electromagnetic Funnel Use for Stirring Up Disperse Particles into the Crystallizer of a Continuous Casting Facility

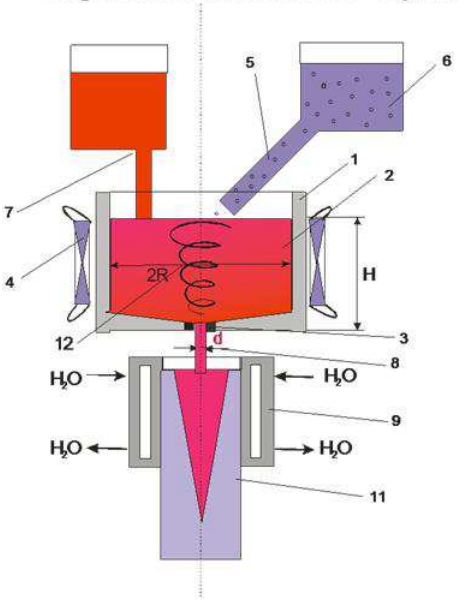

1 - tundish with the melt
2 - molten metal
3 – drain hole
4 – RMF inductor
5 – chute
6 – reservoir with particles
7 – tundish
8 - jet of melt
9 – crystallizer
10 – liquid zone of the ingot
11 – ingot
12 - funnel

13

Titanium Matrix Composites
(currently produced only by powder metallurgy)

- Liquid metal levitation in high frequency AC field
- Stabilization by superimposed DC magnetic field

14

Ceramic reinforcement

- Saffil fiber (Al2O3), Al2O3 particle
- SiC particle and fiber
- Carbon fiber
- Glass fiber
- Boron fiber

15

Applications

- **Automotive and heavy goods vehicle:**
  Bracing systems, piston rods, frames, piston, piston pins, valve spring cap, brake discs, disc brake calliper, brake pads, cardan shaft
- **Military and civil air travel:**
  Axle tubes, reinforcements, blade and gear box casing, fan and compressor blades; Turbine blades
- **Aerospace industry:**
  Frames, reinforcements, aerials, joining elements
- **Energy techniques (electrical components and conducting materials):**
  Carbon brushes ; Electrical contacts; Super conductor
- **Other applications:**
  Spot welding electrodes; Bearings

16

Liquid gallium jet–plasma interaction studies in ISTTOK tokamak

R.B. Gomes[a], H. Fernandes[a], C. Silva[a], A. Sarakovskis[b], T. Pereira[a], J. Figueiredo[a], B. Carvalho[a], A. Soares[a], P. Duarte[a], C. Varandas[a], O. Lielausis[b], A. Klyukin[b], E. Platacis[b], I. Tale[b] and A. Alekseyv[c]

[a]Associação EURATOM/IST, Instituto de Plasmas e Fusão Nuclear/IST, Av. Rovisco Pais, No. 1, 1049-001 Lisboa, Portugal

[b]Association EURATOM/University of Latvia, Institute of Solid State Physics, 8 Kengaraga Str., LV-1063 Riga, Latvia

[c]TRINITI Troitsk, Moscow reg. 142190, Russia

Available online 28 January 2009.

Abstract

Liquid metals have been pointed out as a suitable solution to solve problems related to the use of solid walls submitted to high power loads allowing, simultaneously, an efficient heat exhaustion process from fusion devices. The most promising candidate materials are lithium and gallium. However, lithium has a short liquid state temperature range when compared with gallium. To explore further this property, ISTTOK tokamak is being used to test the interaction of a free flying liquid gallium jet with the plasma. ISTTOK has been successfully operated with this jet without noticeable discharge degradation and no severe effect on the main plasma parameters or a significant plasma contamination by liquid metal. Additionally the response of an infrared sensor, intended to measure the jet surface temperature increase during its interaction with the plasma, has been studied. The jet power extraction capability is extrapolated from the heat flux profiles measured in ISTTOK plasmas.

PACS classification codes: 52.55.F; 52.40.Hf; 28.52.Fa

Article Outline

1. Introduction

The materials currently used in large size fusion devices are submitted to very high thermal loads (up to the GW/m^2 during off-normal events). Due to the high erosion levels and thermal stress produced by such power loads, the plasma facing components are likely to require frequent replacement. This question has recently boosted the interest in the research of liquid metals which could be successfully used to overcome these

problems. The possibility to perform a permanent renewal of liquid surfaces has been pointed out as one adequate solution for both the protection of solid walls and an efficient power exhaust process from fusion plasmas [1]. Among a set of several liquid metals, lithium has shown the best compatibility with fusion plasmas (due to its low Z) as well as a remarkable hydrogen retention properties which allow a low recycling operation with the corresponding enhancement in plasma performance [2], [3] and [4]. However, lithium remains in liquid state in a shorter temperature range than gallium which has essentially better thermal properties and lower vapor pressures (gallium reaches a 10^{-4} mbar vapor pressure at 890 °C, while the same value is achieved by lithium at 400 °C [5]). To explore further these properties, ISTTOK, a tokamak with main parameters: R = 0.46 m, a = 0.085 m, B_T = 0.45 T, $\bar{n}_e(0) = 5 \times 10^{18}$ m^{-3}, $T_e(0)$ = 150 eV, $I_P \sim 6$ kA an $V_{loop} \sim 3$ V, is being used to study the interaction of free flying, fully formed liquid gallium jets with the plasma. The main motivation for this work is based on the rather scarce number of studies on gallium interaction with tokamak plasmas. The only known other experiment was performed in T3-M device using a liquid metal droplet curtain as a limiter [6]. This paper presents some of the results obtained in ISTTOK, as well as the evaluation of the jet surface temperature increase expected for this interaction.

2. Experimental setup

A detailed description of the liquid metal loop installed on ISTTOK to inject gallium at the plasma edge has been done in [7]. Fig. 1 shows details of the implemented setup in the vicinity of the plasma–jet interaction region. The jets are generated by hydrostatic pressure, have a 2.3 mm diameter and a 2.5 m/s flow velocity. The liquid metal injector has been built from a ¼″ stainless steel pipe reduced to a suitable shaping nozzle and allows the positioning of the jet inside the tokamak chamber, within a 13 mm range ($59 < r < 72$ mm). The pressure required to generate a stable, vertical jet is generated by a 1.3 m height liquid metal column. The setup parameters have been chosen to ensure a 13 cm break-up-length (continuous part of the jet, before its spontaneous decomposition into droplets, due to Rayleigh instability). A detailed characterization of the produced jets is presented in [8].

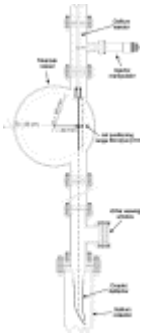

Full-size image (43K)

Fig. 1. Schematic cross-section of the implemented setup in the vicinity of the plasma–jet interaction region.

3. Influence of a gallium jet on ISTTOK plasmas

One of the objectives of this work was to assess the feasibility of tokamak discharges interacting with gallium jets and studying their influence on the plasma parameters. ISTTOK tokamak is equipped with one fully poloidal graphite limiter (FPL) placed at r = 85 mm radius which acts as the main limiting surface during the operation with the gallium jet. A comparison of the main plasma parameters (V_{loop}, I_p, $\bar{n}_e$), for consecutive discharges, with and without liquid metal jets in the chamber has been performed with injection at several radial positions (r = 60, 65 and 70 mm). Typical results, including the radiated power in the UV and visible range, are shown in Fig. 2, for an injection position of r = 65 mm. In this figure radiation losses data was measured by silicon p–n bolometers (IRD Inc. AXUV100 bolometer, integrating light from 1 to 100 nm for UV band, and IRD Inc. UVG100 for the 300 to 900 nm range for visible) oriented along a vertical viewing cord looking towards the chamber center and located at a toroidal angle of $\phi = \phi_{jet} + 195°$. Those measurements clearly show that there are no significant changes in the discharge parameters, particularly in the radiated power demonstrating only a weak interaction between plasma and gallium. The good reproducibility observed from discharge to discharge does not seem to indicate a significant increase in the plasma impurity content or a contamination of the ISTTOK chamber. No evidences of disruption induced by liquid metal had been noticed during the experiments even in the presence of macroscopic size (~1 mm radius) gallium droplet in the discharge [9].

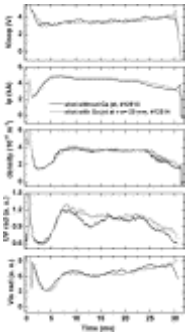
Full-size image (60K)

Fig. 2. Main plasma parameters and radiated power for discharges with and without gallium in the chamber.

In spite of these observations, the release of gallium due to the plasma–liquid metal jet interaction has been clearly identified looking at the plasma emission in the spectral region close to a characteristic wavelength of that element (Fig. 3). This spectrum was obtained using a ½ m imaging spectrograph. The collection optics for this diagnostic was based on a single lens objective that focused radiation into a multichannel fiber input and emitted from a region (~5 × 1 cm^2 effective area) of the poloidal plane where the gallium injection was performed. In this measurement the observation was done along a viewing line tangent to the plasma, in the equatorial plane and directed towards the jet position. This diagnostic was able to provide additional information on the gallium and gallium ion species spatial distribution inside the plasma [7]. Fig. 3 shows that the presence of the jet in the chamber generates a pronounced increase in the spectral line emission. This increase is obviously due to the penetration of gallium in the plasma that is rapidly

ionized, close to the jet surface, to higher ionization stages (Ga, Ga^+ and Ga^{2+} ionization potentials are respectively: 6.0, 20.5 and 30.7 eV). The attempts to acquire spectra like the one shown in Fig. 3, from a viewing window located at $\phi = \phi_{jet} + 135°$ have proven themselves to be unfruitful since the intensity of gallium (either neutral or ionized) lines were lower than the sensor detection limit. In any case the obtained results seem to indicate that the influence of the liquid metal jet on the plasma appears to be only a local perturbation since it is only observable at the jet position without any strong signals of plasma performance deterioration. The main reason for this observation is thought to be related to a reduced amount of gallium being released from the jet surface, either by evaporation or sputtering, during the plasma–jet interaction in ISTTOK, when compared to other impurity sources. This is indeed confirmed by the fact that there is no significant increase in the radiated power in UV band when the highest intensity gallium ions line emission occurs in this spectral region [10].

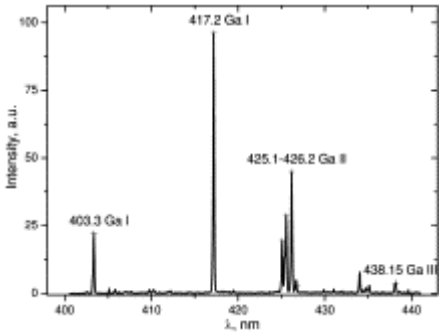

Full-size image (6K)

Fig. 3. Plasma emission spectrum around 420 nm.

4. Gallium jet surface temperature increase analysis

4.1. Evaluation of the gallium jet surface temperature increase

The release of gallium from the jet surface can be due to both particle sputtering and evaporation. The jet is heated during its exposure to plasma and this increase in temperature is the main aspect that influences the evaporation rate. The temperature rise in a planar surface submitted to a power flux density $q(t)$ can be written using the well-known expression [11]:

(1)
$$\Delta T(t) = \frac{1}{\sqrt{\pi \rho C_P \kappa}} \int_0^t \frac{q(t-t')}{\sqrt{t'}} dt';$$

where C_P is the material specific heat, ρ its density and κ its thermal conductivity. This equation is valid provided the heated object thickness is greater than the thermal penetration depth $\delta_{skin} = \sqrt{(\kappa t_{heat}/\rho C_P)}$ where t_{heat} is the heat deposition time. This condition is verified in our case since for a gallium jet in a 30 ms discharge, $\delta_{skin} = 0.64$ mm ($< r_{jet} = 1.15$ mm), assuming that $\rho_{Ga} = 6095$ kg/m^3, $\kappa_{Ga} = 31.7$ W/m K and $C_{PGa} = 380$ J/kg K. It is possible to obtain the expected temperature increase of the gallium jet surface, while passing through the chamber, provided the heat fluxes along its path are known. These parameters have been measured, in ISTTOK using a copper probe

[7]. The heat flux profile shown in Fig. 4(a) was obtained for 9 kW power input ohmic discharges. It is possible to integrate Eq. (1) using the best fit function indicated in this figure and performing the variable transformation: $r \rightarrow \sqrt{(z^2+0.06^2)} \rightarrow \sqrt{((z_0+v_{jet}t)^2+0.06^2)}$, where z is a coordinate along the jet, z_0 the position of an element of fluid, at t = 0 s, and it is assumed that the injector is at a r = 60 mm. Since ISTTOK discharge is short duration the effect of the gravity acceleration has a small contribution to the change in the position of a gallium element of volume present in the chamber and, for simplicity, has been disregarded. The results of these calculations for 16 kW discharges and several flow velocities are presented in Fig. 4(b). It is seen from this figure that the maximum expected temperature increase on the jet surface, in ISTTOK experiment, is about 98 °C. Since at the input the liquid metal is at 75 °C, the maximum temperature it could reach would be 173 °C, for which gallium still has a low vapor pressure ($\sim 10^{-22}$ mbar!). It is also important to stress the behavior of the jet temperature as the flow velocity changes: as expected there is a clear decrease on the liquid metal surface temperature when velocity increases.

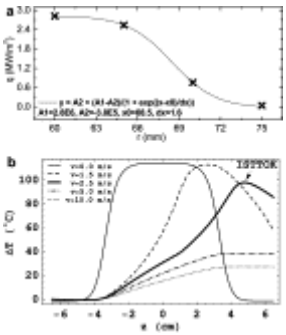

Full-size image (13K)

Fig. 4. (a) Measured plasma heat flux profile in a 9 kW ISTTOK discharge and (b) calculated temperature increase on the jet's surface, for several flow velocities, in a 16 kW discharge.

4.2. Gallium droplets surface temperature monitoring by infrared sensor

The emission of infrared radiation has been successfully used to measure the temperature of liquid lithium surfaces in FTU tokamak [12]. A HgCdTe infrared sensor, with a 6.7 μm cutoff wavelength, is being used in ISTTOK to monitor the radiation emitted by gallium droplets, after liquid metal interaction with the plasma, aiming at studying the power exhaustion capability of such thin jets. Measurements are performed at the viewing window schematically represented on the lower part of Fig. 1. The observation direction is perpendicular to the poloidal plane (in fact perpendicular to the direction represented in Fig. 1). At that distance from the chamber ($\sim$48 cm from the equatorial plane) the gallium jet is already in droplet form and has reached thermal equilibrium since heat propagates about 3 mm (> droplet radius) before reaching that viewing cord. As such, the average power extracted by the gallium jet can be deduced from the specific heat definition by:

(2)
$$\bar{q} = \bar{m} C_{PGa} \Delta T$$

where $\bar{q}$ is the average input power, $\bar{m}$ is the liquid metal mass flow rate and ΔT is the temperature rise, which is intended to be measured in this experiment. A germanium meniscus lens, with broadband antireflection coating, 25.4 mm focal length and 24 mm diameter was used to focus the radiation emitted by gallium droplets on a 1 mm core diameter silver halide optical fiber which, in turn, transmits the radiation to the cryogenically cooled (78 K) sensor.

Measurements with the mentioned device have provided the results shown in Fig. 5. These were obtained, with the collection lens 85 mm away from the droplets position. Each one of the spikes shown in the curves of Fig. 5 corresponds to single droplets. The gray curve in Fig. 5 is a reference shot (no gas) showing the droplet behavior without plasma. This has been obtained with gallium injector at r = 68 mm. This shows that there is a small tilt in the injector direction since it should be centered at r = 60 mm (Nonetheless it should be stressed that this corresponds to an angular shift less than 0.9°). Another important outcome of the measurements, obtained from the analysis of Fig. 5, is that the jet suffers a small (<10 mm) radial displacement due to the influence of the plasma. This is noticed since the droplets are not observed prior to the shot (black curve in Fig. 5, injector at r = 60 mm) and they appear in the collection optics FOV during the discharge time (with the corresponding delay). Previously acquired movies of the jet inside the chamber, during its interaction with the plasma, have not put this fact in evidence since at this location the shift is too small to be clearly identified. The observed increase in the signal amplitude, when compared to the shot without plasma, could only be related to an increase in the gallium jet temperature. It is not possible to provide a value for this parameter since its measurement requires a calibration procedure of the detector which is under development. But it is worthy to mention that for both curves, in Fig. 5, gallium at the injector output was at a temperature close to 75 °C. Unfortunately the sensor response is not linear [12] and this value is not enough to obtain the droplets temperature increase due to the plasma interaction. The low signal amplitude obtained for the data presented in Fig. 5 (a few mV) is related to two factors: (1) the low voltage output of the infrared sensor was connected directly to the tokamak data acquisition system, without being amplified and (2) the sensor response was not the most recommended for the temperature range under consideration. A new three-channel infrared sensor is planned for future measurements, using a more sensitive detector (suitable for lower temperature values, cutoff wavelength of 9 μm) and higher spatial resolution which will allow following the motion of the gallium droplets along the referred radial displacement.

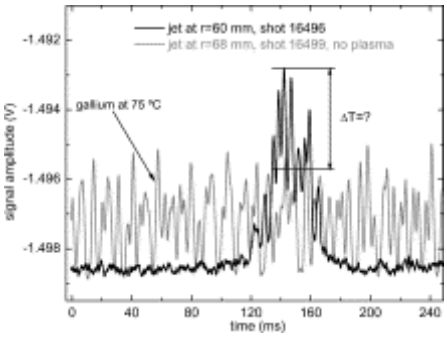

Full-size image (35K)

Fig. 5. Signal from the infrared sensor with and without plasma.

5. Summary

The interaction of the liquid gallium jet with ISTTOK plasmas has no significant effect on the discharge behavior and no severe effects on the main plasma parameters. The time evolution of visible radiation from gallium characteristic spectral lines close to the jet and at one toroidally symmetric position shows that plasma-liquid metal interaction has only a local effect. This work proved the technical feasibility of gallium jets interacting with plasmas. Although the expected temperature increase of the jet surface had been estimated, the experimental measurements still require an ongoing calibration procedure to provide further insight in the jet power exhaustion capability.

Acknowledgments

This work has been carried out within the framework of the Contract of Association between the European Atomic Energy Community and 'Instituto Superior Técnico'. Financial support was also received from 'Fundação para a Ciência e Tecnologia' and 'Programa Operacional Ciência, Tecnologia, Inovação do Quadro Comunitário de Apoio III'.

References

[1] M.A. Abdou and The APEX team, *Fus. Eng. Des.* **45** (1999), p. 145. Abstract | **Article** | PDF (1624 K) | View Record in Scopus | Cited By in Scopus (80)
[2] R. Majeski, R. Doerner, T. Gray, R. Kaita, R. Maingi and D. Mansfield *et al.*, *Phys. Rev. Lett.* **97** (2006), p. 075002. **Full Text** via CrossRef
[3] V. Pericoli-Ridolfini, M.L. Apicella, G. Mazzitelli, O. Tudisco, R. Zagórski and The FTU team, *Plasma Phys. Control. Fus.* **49** (2007), p. S123. **Full Text** via CrossRef
[4] D.K. Mansfield, D.W. Johnson, B. Grek, H.W. Kugel, M.G. Bell and R.E. Bell *et al.*, *Nucl. Fus.* **41** (2001), p. 1823. **Full Text** via CrossRef | View Record in Scopus | Cited By in Scopus (24)
[5] R.E. Honig and D.A. Kramer, *RCA Rev.* **30** (2) (1969), p. 285.
[6] S.V. Mirnov and V.A. Evtikhin, *Fus. Eng. Des.* **81** (2006), p. 113. **Article** | PDF (270 K) | View Record in Scopus | Cited By in Scopus (5)
[7] R.B. Gomes, H. Fernandes and C. Silva *et al.*, *Fus. Eng. Des.* **83** (2008), p. 102. **Article** | PDF (1056 K) | View Record in Scopus | Cited By in Scopus (4)
[8] R.B. Gomes, H. Fernandes and C. Silva *et al.*, *AIP Conf. Proc.* **875** (2006), p. 66. View Record in Scopus | Cited By in Scopus (0)
[9] R.B. Gomes, H. Fernandes, C. Silva and A.C.A. Figueiredo, *IEEE Trans. Plasma Sci.* **36** (4) (2008), p. 1086. **Full Text** via CrossRef | View Record in Scopus | Cited By in Scopus (1)
[10] T. Shirai, J. Reader, A.E. Kramida and J. Sugar, *J. Phys. Chem. Ref. Data* **36** (2007), p. 509. **Full Text** via CrossRef | View Record in Scopus | Cited By in Scopus (6)
[11] H.S. Carslaw and J.C. Jaeger, Conduction of Heat in Solids (2nd Ed.), Oxford University, Oxford (1959).
[12] A. Alekseev, V. Lazarev, Ya. Gorbunov, G. Mazzitelli, M.L. Apicella, G. Maddaluno, 33rd EPS Conference on Plasma Physics (Rome, Italy, 2006), p. 1.162.

Titāna ražošanas tehnoloģijas izstrādāšana, bāzējoties uz savstarpēju titāna tetrahlorīda un metāliskā magnija tvaiku savstarpēju mijiedarbību

Šobrīd pasaulē metālisko titānu ražo, izmantojot garu un dārgu ražošanas procesu. Tas paredz kā izejvielu izmantot titāna rūdu, starpposmā ražojot titāna sūkli.

Tradicionālā titāna ražošanas pamatā ir titāna tetrahlorīda reakcija ar magniju:

$$\frac{1}{2}\mathrm{TiCl_4} + \mathrm{Mg} \rightarrow \frac{1}{2}\mathrm{Ti} + \mathrm{MgCl_2}$$

94,86 + 24,32 -> 23,95 + 95,23 (molekulu masas)

Rūpniecībā tiek izmantotas iekārtas, kuru ražība viena cikla laikā sastāda 3-5 tonnas titāna. Dažādas iekārtas var atšķirties ar nelielām tehniska rakstura niansēm, bet visu iekārtu pamatā ir sekojošas galvenās sastāvdaļas un mezgli: krāsns, reaktors /retorte/, titāna tetrahlorīda ievadīšanas mezgls, magnija ievadīšanas mezgls, magnija izvadīšanas mezgls, kā arī ražošanas procesa kontroles un regulēšanas aparatūra.

Ražošanas process sastāv no atsevišķām operācijām, kuras atkārtojas katrā atsevišķā ciklā. Hermētisku reaktoru /retorti/ ievieto uzkarsēta krāsnī, atvakuumē un uzpilda ar neitrālu argona gāzi, pievieno minētos uzpildīšanas mezglus. Reaktoru uzpilda ar noteiktu magnija daudzumu, uzkarsē līdz temperatūrai 800-850°C un ievada titāna tetrahlorīdu. Procesam beidzoties retorti atdzesē, izceļ no krāsns un nodod nākošai operācijai, proti, iegūto titāna sūkli atdala no magnija un hlorīda paliekām to separējot vakuuma apstākļos. Jāatzīmē, ka procesa gaitā stingri jāseko temperatūras režīmam reaktorā, jo pie augstām temperatūrām titāns un dzelzs /Fe/ veido sakausējumu ar kušanas temperatūru 1085°C. Tas var izsaukt reaktora sienu bojāšanos, kas savukārt var novest pie avārijas.

- Apskatītais titāna iegūšanas process ir ciklisks un tā praktiskā realizācija izsauc nopietnas neērtības.
- Arī piedāvātā ražošanas procesā kā izejviela tiek izmantots titāna tetrahlorīds un magnijs, tikai titāna tetrahlorīds tiek reducēts ar magniju speciālā ar niobiju plaķētā reaktorā /retortē/ - bet jau minēto komponenšu tvaiku stāvoklī.
- Piedāvātā projekta galvenais mērķis ir izstrādāt nepārtrauktu titāna stieņu iegūšanas metodi un eksperimentāli parādīt tās realizācijas tehnisku iespēju.
- Dotais paņēmiens (metode), reducējot titāna tetrahlorīdu ar magniju to tvaiku stāvoklī ietver:
    - temperatūras uzturēšanu reaktora reakcijas zonā augstāk par metāliskā titāna un metāla-reducētāja vārīšanās temperatūru, pie kam nākošajā etapā /ja projekta rezultāti būs pozitīvi/ ir paredzēts reaktoru izveidot elektriskās loka krāsns veidā;
    - titāna tetrahlorīda un metāliskā magnija vienlaicīgu padevi uz reaktoru reakcijas īstenošanai, uzturot metālisko titānu vai metāliskā titāna un blakusproduktu sakausējumu izkausētā veidā;
    - metāliskā titāna savākšanu reaktora apakšējā daļā.

Eksperimentālais stends

Magnija iztvaikošanas temperatūra ir pāri par 1100°C, pie tam titāna tetrahlorīda un magnija reakcija ir eksotermiska un temperatūra reaktorā var pārsniegt 1400°C. Tāpēc reaktoru ir jāizgatavo no karstumizturīga materiāla. Piedāvātajā konstrukcijā reaktors izgatavots no niobija - cirkonija sakausējuma, fig.1. Galvenā problēma bija nodrošināt reaktoram vakuuma apstākļus. Citiem vārdiem, reaktors bija jāievieto speciālā no

nerūsējoša tērauda izgatavotā korpusā, kura tilpums ir piepildīts ar inerto gāzi, vai arī no tā izsūknēta atmosfēra /gaiss /.

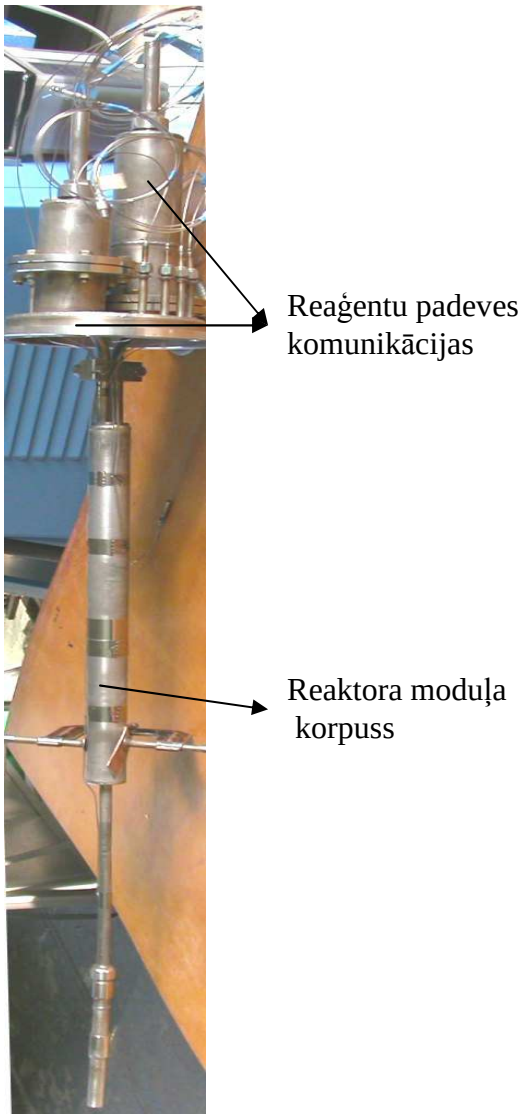

Fig. 1.

Reaktora modelis

Eksperimentālais stends, kura galvenie mezgli ir magnija tīģelis ar izkausētu magniju, titāna tetrahlorīda trauks , magnija hlorīda trauks reakcijas produktiem , hlorīda tvaiku tilpums, reaktora korpuss un vakuumsūknis ir parādīts fig.2., bet stenda principiālā shēma, fig.3.

Darbi ar reaģentiem pie tam pie temperatūrām 1200 – 1400C^2 prasa noteiktu piesardzību un tika veikti izolētā telpā aprīkotā ar specventilāciju un specapģērbos.

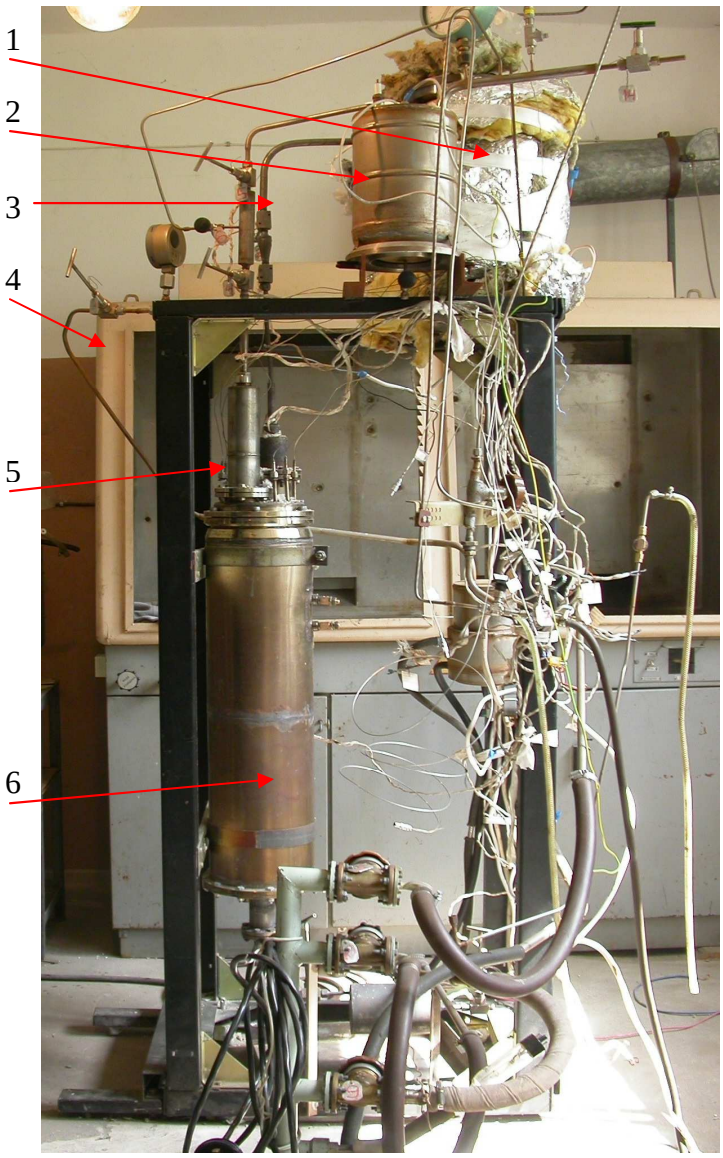

Fig. 2.

Eksperimentālais stends

1- magnija tīģelis; 2- titāna tetrahlorīda tvertne; 3- magnija padeves komunikācijas; 4- titāna tetrahlorīda padeves komunikācijas; 5- reaktora moduļa aizsargapvalks; 6- kondensators

LU Fizikas institūta dzīvsudraba laboratorija

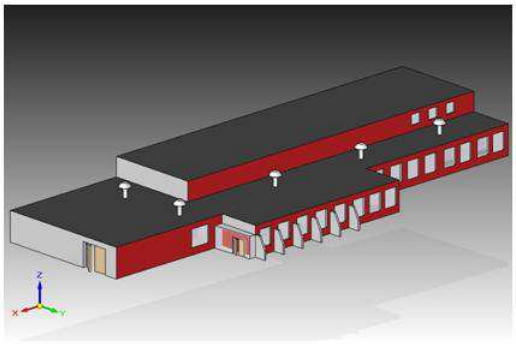

Mercury laboratory at Institute of Physics
University of Latvia

Total area of Mercury lab 1400 sqm

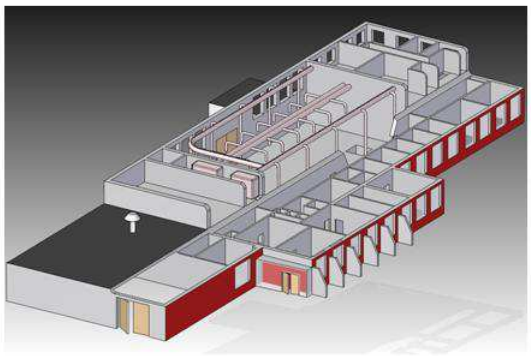

Mercury laboratory at Institute of Physics

Experimental hall of Mercury laboratory

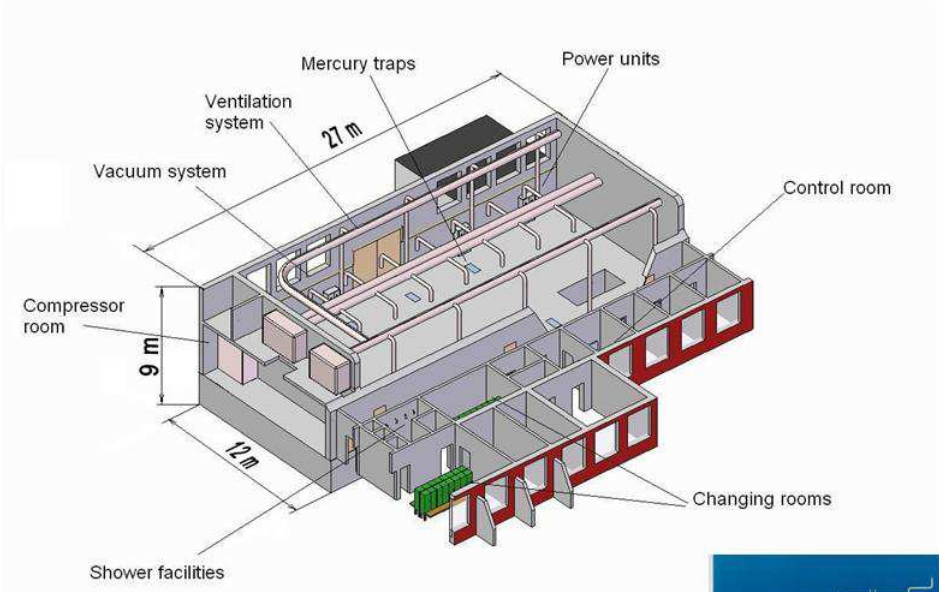

Principal layout Spallation Neutron Source (SNS)

MERCURY LOOP DN 100

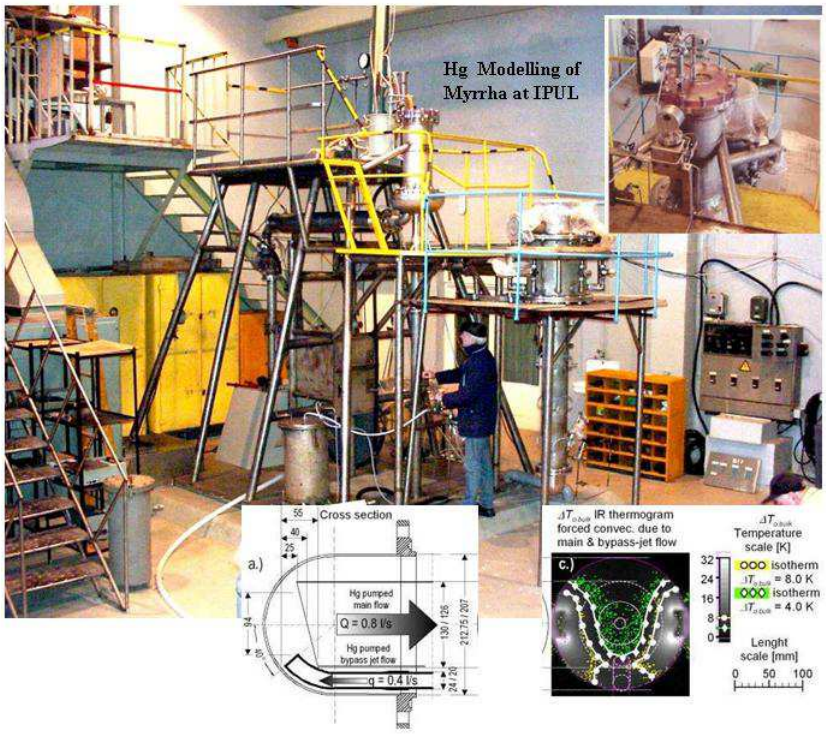

Test of mock-up of MEGAPIE target in scale 1:1

Tests of 180^0 bend target

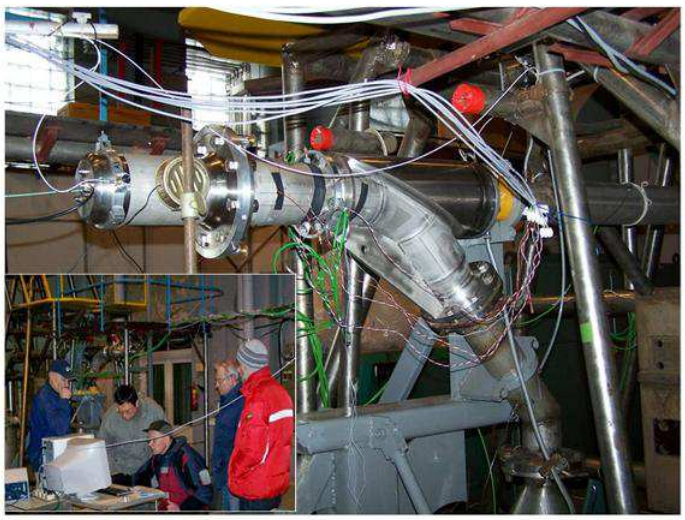

Principal diagram of ESS target Hg-He loop

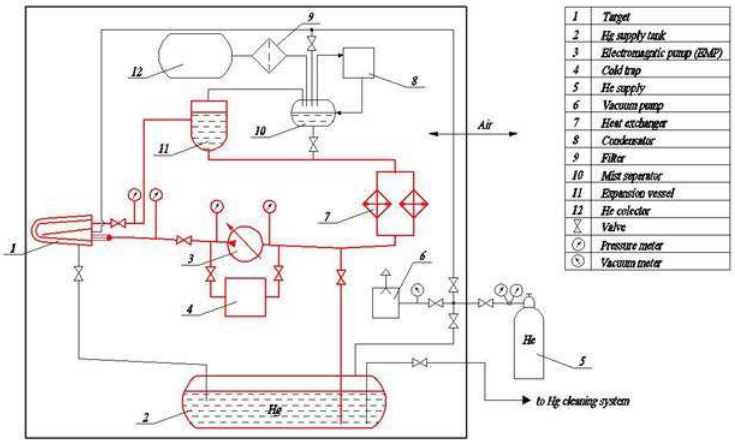

PRINCIPLE SCHEME OF MERCURY PURIFICATION STAND

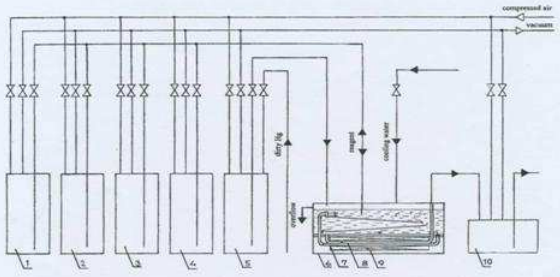

1 - tank NaOH; 2 - tank HNO_3; 3 - tank C_2H_5OH; 4 - tank H_2O; 5 - tank Hg;
6 - equipment for Hg purification; 7 - circulating channel; 8 - pumping channel;
9 - MHD pump; 10 - pure Hg tank.

STAND IN THE Hg LABORATORY OF THE INSTITUTE OF PHYSICS

Quantity of Hg under cleaning, kg	- 50
Time of cleaning, min	- 90 to 30
Voltage, V	- 380, 220
Active power, kW	- 2.5
Mass, kg	~ 400

International Journal of Heat and Mass Transfer 52 (2009) 5302–5308

Contents lists available at ScienceDirect

International Journal of Heat and Mass Transfer

journal homepage: www.elsevier.com/locate/ijhmt

Surface cooling based on the thermomagnetic convection: Numerical simulation and experiment

D. Zablotsky *, A. Mezulis, E. Blums

Institute of Physics, Latvian University, Miera Str. 32, Salaspils-1 LV-2169, Latvia

ARTICLE INFO

Article history:
Available online 26 August 2009

Keywords:
Ferrofluid
Thermomagnetic convection
Nusselt number
Thermosiphon
Cooling

ABSTRACT

In this paper we present the results of our numerical and experimental investigation of thermomagnetic convection in a temperature sensitive ferrofluid under the influence of strong non-uniform magnetic field. The convection is studied in a rectangular cell with permanent magnets attached to the cell walls. When the cell is heated from below, the observed intensification of heat transfer is significantly higher than that in the case of simple thermogravitational convection. The predictions of the numerical simulations are compared with the experimental results with good correspondence.

1. Introduction

Ferrofluids are stable colloidal suspensions of nanoscale ferromagnetic particles suspended in non-magnetic carrier, usually water or organic oil. The diameter of nanoparticles is ca. 10 nm. In order to prevent coagulation, the particles are sterically stabilized with layers of the surfactant. Due to their composition, such fluids exhibit superparamagnetic properties, which introduces into conventional transport processes an additional control parameter – the magnetic field, leading to appearance of new interesting effects.

The temperature dependence of magnetization causes appearance of a non-uniform body-force in differentially heated volume of ferrofluid, subjected to externally applied or internal magnetic field gradients [1]. The resulting convective motion – thermomagnetic convection – is in many ways similar to the thermogravitational one. In order to achieve high magnitude of driving force and intensive convection, special temperature-sensitive ferrofluids with high temperature dependence of magnetization as well as strong magnetic field gradients should be used.

The practical interest in thermomagnetic convection is motivated by its high potential for small scale cooling devices. The cooling of hot surfaces is an outstanding problem in a wide range of engineering and electronics applications. In most cases the classical gravity convection is unable to sustain adequate heat transfer efficiency in small scale setups or reduced gravity conditions, therefore forced convection is used in most technical applications. On the other hand, in strong magnetic fields the intensity of thermomagnetic convection can significantly exceed that of the pure thermogravitational. Compared to active setups currently employed in electronics, the relative simplicity of passive thermosiphon type ferrofluid cooling devices, based on self-regulating and self-sustaining nature of the thermomagnetic convection, and the absence of moving parts make it a highly interesting topic.

Since the prediction of Finlayson [2] of a novel convective instability in ferrofluids, leading to the thermomagnetic convection, a significant number of theoretical and experimental investigations have been performed in this area related to different geometries: Rayleigh–Bernard configuration, rectangular enclosure [3], cylinder [4–6], cube [7], partitioned cavity [8], etc. – and magnetic field configurations – homogenous distribution, constant field gradient [9], field of a line dipole [10] and others – confirming that the increase of convective heat transfer efficiency takes place under the applied magnetic field. Several attempts have been made to approach efficient cooling based on the ferrofluid convection both with magnetic coils and permanent magnets. Nakatsuka et al. [11] have investigated heat transfer characteristics of a heat pipe containing water-based magnetic fluid and measured 13% increase of heat transfer efficiency caused by non-uniform magnetic field. Yamaguchi et al. [12] numerically and experimentally investigated thermomagnetic convection in a rotation disk and came to a conclusion that vortexes impede convective heat transfer at high magnetic fields. Fumoto et al. [13] and most recently Li et al. [14,15] have thoroughly characterized the performance of a permanent magnet based miniature convection loop filled with temperature-sensitive ferrofluid, confirming the characteristic features of the thermomagnetic convection – stability and self regulation. For additional effect, in the latter work the Curie point of the ferrofluid was tuned to be within the operational temperature range.

* Corresponding author. Tel.: +371 67944664; fax: +371 67901214.
E-mail address: dmitrijs.zablockis@gmail.com (D. Zablotsky).

0017-9310/$ - see front matter © 2009 Elsevier Ltd. All rights reserved.
doi:10.1016/j.ijheatmasstransfer.2009.08.001

Nomenclature

c_p	heat capacity at constant pressure (J kg^{-1} K^{-1})
d	diameter of the cylindrical heater (m)
f	Kelvin's force (N)
g	gravitational acceleration (m s^{-2})
H	magnetic field intensity (H m^{-1})
h'^{-}	magnet shift (m)
I	current to the heater (A)
k_B	Boltzmann constant (=1.38 × 10^{-23} J K^{-1})
l	length of the heater (m)
L	characteristic distance (m)
m	magnetic moment of the ferroparticle (A m^2)
M	magnetization (A m^{-1})
M_{ref}	reference magnetization (A m^{-1})
M_S	saturation magnetization (A m^{-1})
Nu	Nusselt number
Pr	Prandl number
q	heat flux density (W m^{-2})
q_w	heat flux density through the heaters surface (W m^{-2})
Ra	gravity Rayleigh number
Re	Reynolds number
Rm	magnetic Rayleigh number
s_w	heater surface (m^2)
t	real time (s)
T	temperature (K)
T_{ref}	reference temperature (K)
u	vertical flow velocity (m s^{-1})
U	voltage on the heater (V)

Greek symbols

α	convective heat exchange coefficient (W/m^2 K)
β_m	pyromagnetic coefficient (K^{-1})
β_T	thermal expansion coefficient (K^{-1})
η	dynamic viscosity of the working liquid (N s m^{-2})
λ	thermal conductivity of the working liquid (W m^{-1} K^{-1})
μ_0	vacuum magnetic permeability (=4π × 10^{-7} H m^{-1})
ν	kinematic viscosity of the working liquid (m^2 s^{-1})
ρ	solvent density (kg m^{-3})
φ	particle volumetric concentration

The main challenge in designing a cooling device, based on the thermomagnetic convection, is achieving sufficiently high efficiencies of heat transfer, which requires special ferrofluids with high temperature sensitivity of magnetization. Prospective candidates for heat transfer applications are ferrofluids based on Mn–Zn nanoparticles, characterized by higher value of the pyromagnetic coefficient than widely used ferrite ones [16].

In this paper we report the results of our investigations of thermomagnetic convection in a rectangular convection cell filled with a temperature sensitive ferrofluid containing Mn–Zn nanoparticles. The aim of our research is to determine the intensity of convective motion and sustainable efficiency of the heat transfer due to thermomagnetic convection caused by sufficiently strong magnetic field. The experimental results are complemented by the numerical simulations.

2. Setup

The thermomagnetic convection has been investigated in a rectangular ferrofluid cell, made from plexiglass (Fig. 1) with dimensions 100 × 15 mm and 150 mm in height.

From both sides the cell is enclosed by strong permanent magnets 50 × 100 mm, begirded with a magnetic circuit. Two thin non-magnetic rigid ribs, positioned along the sides of the magnets, separate the central part of the cell. In order to reduce the heat loss from the large sidewalls, the cell is put in the plastic foam.

The working medium is a temperature sensitive ferrofluid DF-67K with Mn–Zn nanoparticles suspended in tetradecane. Magnetic granulometry measurements [5] at different temperatures have shown almost linear dependency of the magnetization in a wide temperature range between 20 and 250 °C and large value of the pyromagnetic coefficient. The main physical parameters of DF-67K and its solvent are summarized in Table 1. The temperature gradient, necessary for appearance of the thermomagnetic convection, is provided by the water reservoirs with constant temperature, placed at the upper and lower ends and separated from the surface of the cell with two semi-conductive 3 mm thick plates. The volume of ferrofluid is heated from the bottom and cooled from the top.

The applied magnetic field, provided by the permanent magnets, has been measured in the mid-plane of the convection cell along

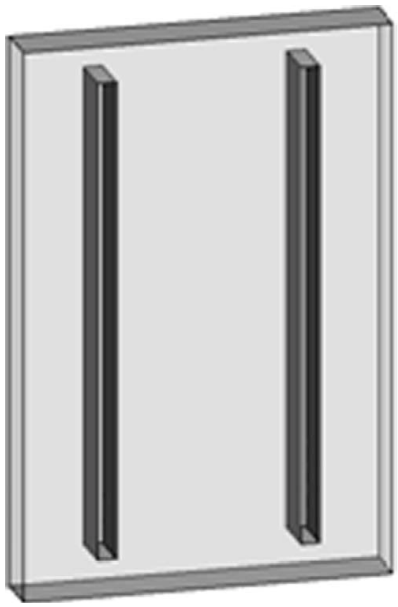

Fig. 1. Schematic view of the convection cell.

Table 1
Parameters of the ferrofluid DF-67 K.

Parameter	Value	Units
Solvent density	976	kg m^{-3}
Dynamic viscosity	0.006	Pa s
Specific heat capacity	2190	J kg^{-1} K^{-1}
Thermal expansion coefficient	9.33 × 10^{-4}	K^{-1}
Thermal conductivity	0.14	W m^{-1} K^{-1}
Particle diameter	~10	nm
Volumetric concentration	6	%
Saturation magnetization	1.2 × 10^6	A m^{-1}
Pyromagnetic coefficient	0.0028	K^{-1}

direction of the vertical axis of cell in three locations: at points A (at the center, $x = 0$ mm), B (along the side-edge of the magnet, $x = 25$ mm) and C ($x = 40$ mm). The results together with composed distribution of the magnetic field in the cell are shown in Fig. 2.

The strongest magnetic field in the cell volume between the poles is 640 kA m^{-1}, and its vertical gradient at the edges of poles is approximately 25,000 kA m^{-2}. The vertical separating ribs prevent the flow of fluid in lateral direction, effectively forming a thermomagnetic pump.

3. Numerical simulation

3.1. Governing equations

The external magnetic field in question is sufficiently strong to be considered constant, and all perturbations due to the ferrofluid motion can be neglected. The magnetic force, acting on the differentially heated non-conducting magnetic liquid, is described by Kelvin's body force:

$$\mathbf{f} = \mu_0(\mathbf{M}\nabla)\mathbf{H} \quad (1)$$

The magnetization of the ferrofluid is temperature-dependant. Introducing the linear equation of state:

$$M(T) = M_{ref}(1 - \beta_m(T - T_{ref})) \quad (2)$$

where $\beta_{ref} = \frac{1}{M_{ref}}\frac{\partial M}{\partial T}\Big|_{T_{ref}}$ is the pyromagnetic coefficient. Reference magnetization has been calculated according to the single-parameter Langevin approximation:

$$M_{ref} = \varphi M_S \cdot L(\xi), \psi \quad L(\xi) = \frac{1}{\tanh(\xi)} - \frac{1}{\xi}, \psi\xi = \frac{\mu_0 m_d H}{k_B T} \quad (3)$$

The flow of the magnetic fluid is governed by the incompressible Navier–Stokes equation, continuity equation and temperature equation without viscous dissipation. We have used the Boussinesq approximation and linear equation of state for the temperature dependence of density:

$$\rho(T) = \rho_{ref}(1 - \beta_T(T - T_{ref})) \quad (4)$$

Without the magnetic field, a convective motion in the cell can take place only due to buoyancy effects. In this regime the gravity Rayleigh number

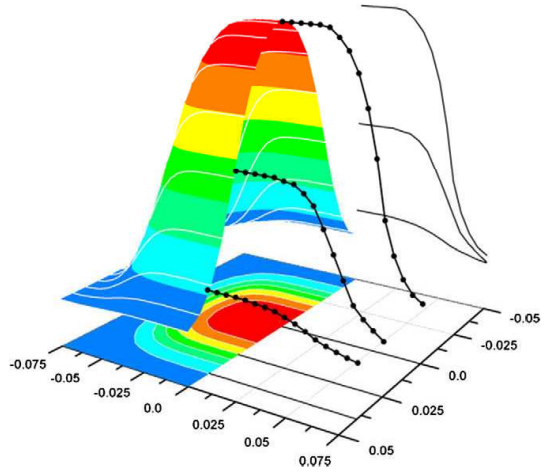

Fig. 2. Measured and reconstructed distribution of the magnetic field provided in the cell by permanent magnets.

$$Ra = \frac{\rho c_p L^3 \Delta T}{\eta\lambda}\beta_T \rho g \quad (5)$$

is much less than critical value for the onset of turbulence, therefore laminar convection takes place. This type of convection can be simulated directly within a reasonable timescale with conventional DNS approach.

By analogy with the thermogravitational convection, the magnetic Rayleigh number is introduced for the thermomagnetic convection

$$Rm = \frac{\rho c_p L^3 \Delta T}{\eta\lambda}\mu_0 \beta_m M \nabla H \quad (6)$$

When a temperature sensitive ferrofluid is subjected to a strong magnetic field gradient, the magnetic Rayleigh number even for relatively small temperature differences proves to be orders of magnitude larger than the gravity Rayleigh number, and exceeds the critical threshold for the onset of turbulence. With the present setup at temperature difference 20 K a conservative estimation gives $Ra \approx 5 \times 10^6$ and $Rm \approx 5 \times 10^9$.

In order to simulate turbulent convection we have used RANS equation solver implemented in ANSYS CFX with SST k–w two-equation closure model.

The magnetic force was introduced via momentum source – this approach has been thoroughly validated by Snyder et al. [17].

Due to non-steady nature of thermal and thermomagnetic convection, transient simulations are required. All calculations were started from zero-velocity initial conditions and advanced with the time step varying from 0.1 to 50 ms. Transient averaging of velocity and temperature fields has been performed in order to distinguish convective patterns after averaged heat flux through the ferrofluid cell reached equilibrium. All parameters have been varied with the applied temperature difference 20 K, except when the temperature difference was changed itself.

3.2. Results

Calculated averaged velocity and temperature distributions in the ferrofluid cell at temperature difference over the full height of magnetic fluid volume $\Delta T = 20$ K, heated from below and cooled from above, are shown in Fig. 3a. The structure of the flow and position of the circulation areas are similar to the ones observed at lower Rayleigh and magnetic Rayleigh numbers in a laminar regime. The inner section of the cell between the areas of largest magnetic field gradient is occupied by two (considering symmetry) large recirculation areas, whereas smaller circulation areas are present at the lower end of the separating rib and in the upper corner of the cell.

The temperature distribution corresponding to this case is presented in Fig. 3b. The inner section of the convection cell between the separating ribs is occupied by a downgoing flow of slightly colder ferrofluid sucked in by the magnetic field. The warmer fluid, heated at the lower surface, is pushed out of the magnetic field to the outer section of the cell, where it rises along the sidewall due to buoyancy forces.

The averaged velocity profile in the middle of the cell between the separating ribs is shown in Fig. 4. The length-average absolute velocity across the profile is approximately 21 mm s^{-1}. This value will be compared with the experimental results of hot-wire velocimetry.

Another interesting case is when the applied temperature gradient is oriented upwards. In this case the ferrofluid in the convection cell is heated from the top and cooled from the bottom, and the thermomagnetic convection is not aided by buoyancy. Calculated averaged streamlines with the temperature difference 20 K are shown in Fig. 5a, and the corresponding temperature contour

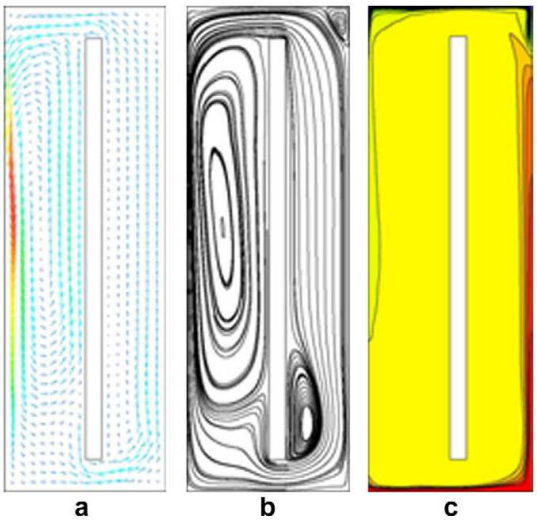

Fig. 3. Calculated averaged velocity and temperature distributions with temperature difference $\Delta T = 20$ K: (a) averaged velocity vectors (b) streamlines (c) temperature distribution, heated from below.

plot in Fig. 5b. The structure of the flow is very similar to the case of temperature gradient oriented downwards, which means that the characteristic features of the flow are determined actually by the magnetic field, and the thermogravitational convection plays a secondary role, as it follows from the estimated ratio of thermogravitational and thermomagnetic Rayleigh numbers.

Additional calculations at other temperature differences have been carried out. Increasing the applied temperature difference between the bottom and top surfaces of the ferrofluid cell to 40 or 80 K splits and suppresses the circulation areas in the inner section of the cell and expands the one near the lower end of the separating rib (Fig. 6).

The temperature profiles in these cases are very similar to the ones at 20 K and are not shown.

The heat transfer efficiency of convection can be characterized by the Nusselt number as a ratio of heat flux through the ferrofluid cell due to convective motion to the one due to heat conduction. We use the relative Nusselt number Nu/Nu_0 instead, defined as a ratio of heat flux through the cell due to thermomagnetic convection to the heat flux due to the thermogravitational convection only, averaged over sufficient time interval. The dependence of

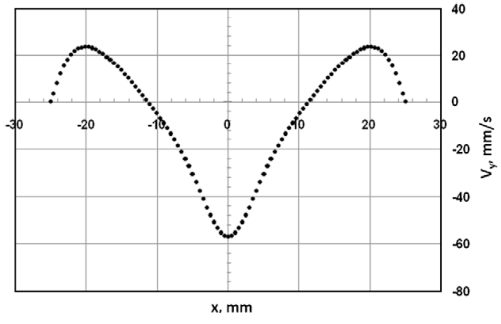

Fig. 4. Averaged velocity profile along the midline of the cell between the separating ribs.

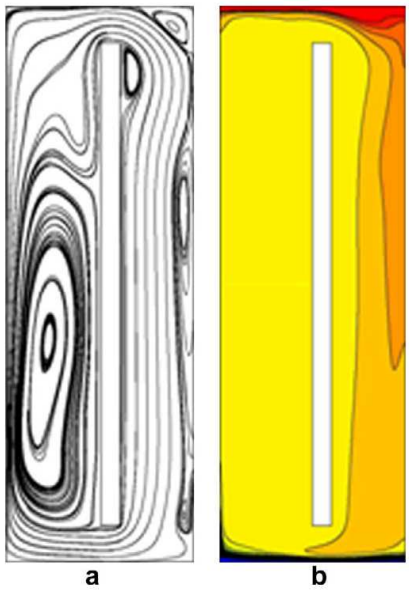

Fig. 5. Calculated averaged velocity and temperature distributions for temperature difference $\Delta T = 20$ K: (a) streamlines (b) temperature distribution, heated from above.

the relative Nusselt number on the applied temperature difference is shown in Fig. 7a.

The heat transfer efficiency slightly decreases with increasing the heat load on the ferrofluid cell. Such an effect may exist due to the change of flow regime at higher applied temperature difference: under action of the magnetic field a transition to the turbulence takes place, leading to different scaling law.

In order to determine the optimal position of the magnetic poles, additional series of calculations has been performed with different magnetic field shifts along the axis of the cell (y-axis), relative to the symmetrical placement. The dependence of the relative Nusselt number on the position of the magnets h' is shown in Fig. 7b. The heat transfer efficiency is significantly increased if the ferrofluid is heated in the area of maximum field gradient. The maximum intensification of convective heat transfer in this series, when the magnet is shifted 20 mm downwards, is approximately 2 times. Further shifting of the magnetic field was prevented by the experimental setup.

4. Experiment

Experimental setup is shown schematically in Fig. 8. In experiments the temperature gradient in semi-conductive 3 mm thick plates, which are placed between convection cell ends and warm/cold water reservoirs, is measured. From these measurements the heat flux density q through the plates is calculated, which leads to obtaining the convective heat exchange coefficient between working liquid and the plates in upper and lower ends of the cell: $\alpha = q/\Delta T$. Experimental setup allows the shift of magnets up and down along the convection cell to search for the best intensification of magnetoconvection by changing heating/cooling ratio at the edges of the magnets.

Experimental results are collected with the aim to compare them with Fig. 7a and b. The only dissimilarity is using the heat exchange coefficient α, which seems to be preferable by its simple measuring technique, instead of Nu.

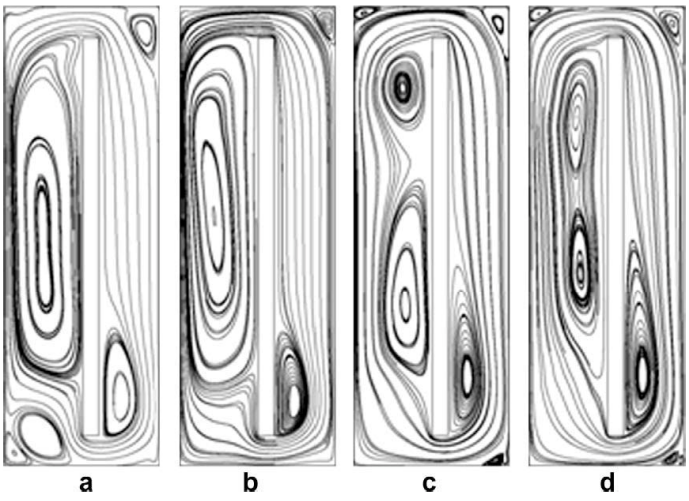

Fig. 6. Calculated averaged velocity: (a) streamlines at $\Delta T = 10$ K (b) streamlines at $\Delta T = 20$ K (c) streamlines at $\Delta T = 40$ K (d) streamlines at $\Delta T = 80$ K, heated from below.

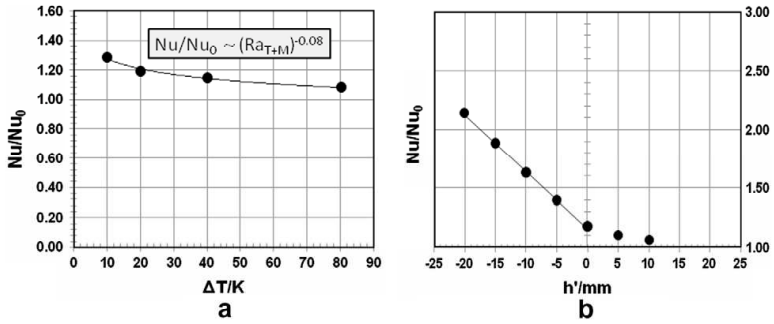

Fig. 7. Intensification of convective heat transfer through the cell (a) at various temperature differences, $h' = 0$ (b) shifted positions of the magnetic field, $\Delta T = 20$ K.

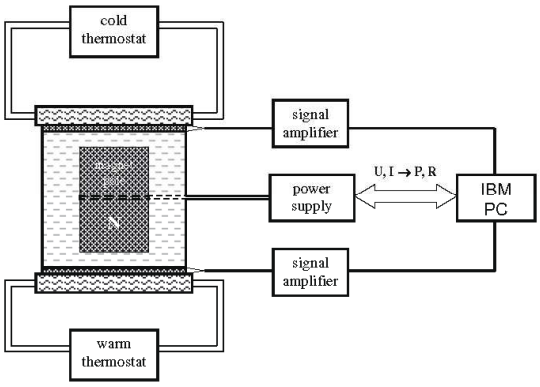

Fig. 8. Experimental setup.

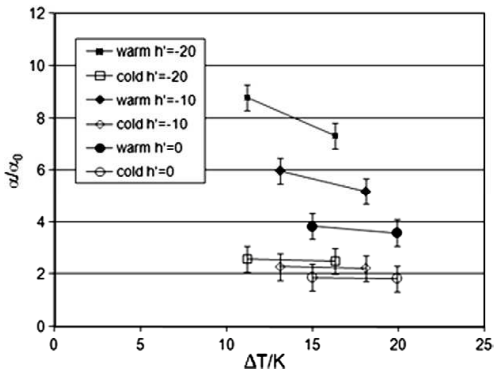

Fig. 9. Measurements of relative heat exchange coefficient α/α_0 vs. the temperature difference ΔT with three magnet positions h'.

Fig. 9 shows the relative heat exchange coefficient α/α_0 as a function of ΔT with three magnet positions. The temperature difference ΔT varies with the magnet shift h' because the experiments are performed at certain temperature difference between the heater and the cooler. Obviously, one must subtract the temperature differences on the semi-conductive plates (~10 K) to obtain ΔT.

In order to save hermetism of the convection cell at acting thermal expansion stresses, in experiments the temperature difference is varied only in a short range, 10 K. It makes no sense to try to obtain curving of a very slight slope within inherent experimental accuracy, therefore taken dependences are linearized.

The difference of the heat exchange at warm and cold ends of the cell can be explained by heat loss through the quite large cell sidewalls. Indeed, the temperature of the laboratory room 15 °C is much closer to that of the cold end 10 °C. During experiments the cell has been put into plastic foam, but as a matter of fact it avoided this effect only partially.

By analogy with Fig. 7b in the theoretical part, Fig. 10 shows determined relative heat exchange coefficient α/α_0 vs. the magnet shift h' at fixed temperature difference $\Delta T = 20$ K.

In Fig. 10 it is clearly seen how strong the heat exchange coefficient depends on the magnet position. More efficient turns to be lower placement of the magnets $h' < 0$, i.e. the magnetic field nearer to the warm end (for the present setup the range of magnet shift is ±20 mm). We get maximal value of the heat exchange coefficient $\alpha_{max} = 47$ W/m^2 K at the warm end, when the magnets are maximally shifted downwards. In the stationary state of this experiment the heat flux density on the warm (i.e. cooled) surface reaches 750 W m^{-2}.

Additional series of measurements regard the small cylindrical heater of diameter $d = 4$ mm, which is placed horizontally between the separating ribs in the middle of the cell. The length of the heater, as well as the distance between the ribs $l = 50$ mm matches exactly that of the magnet, see Fig. 8. The voltage and the current of the heater are measured with a high accuracy. From these measurements the ohmic resistance of the heater is calculated to find out the temperature of the heater body. Also the density of dissipated power through the heater surface can be easily calculated:

$$q_w = \frac{UI}{s_w}\cdot\psi \qquad (7)$$

The governing equation of the laminar flow allows to calculate vertical flow velocity u of the working liquid around the cylindrical heater [18]:

$$Nu = 0.664\sqrt{Re}\sqrt[3]{Pr}\,\psi \qquad (8)$$

where the Reynolds number $Re = \pi\, du/2\nu$ includes searched velocity u, and the Prandl number $Pr = \rho c_p \nu/\lambda$. In contradistinction to the relative Nusselt number, used in the theoretical part of the paper, Eq. (8) considers the conventional Nusselt number $Nu = q_w d/\lambda \Delta T_w$, which is calculated from experimental data U, I, ΔT_w by Eq. (7). Note that ΔT_w is the temperature difference between the surface of the heater and magnetic fluid at the middle of volume.

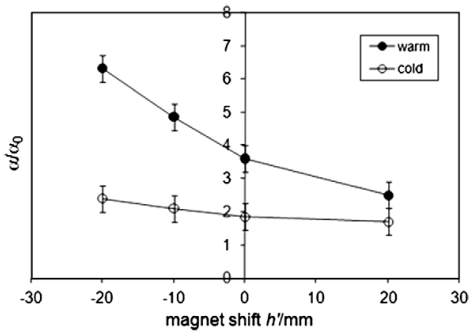

Fig. 10. Dependence of relative heat exchange coefficient α/α_0 on magnet shift: $h' > 0$ means the magnet shift upwards, $h' = 0$ is the central magnet position (as shown in Fig. 8).

Vertical flow velocity measurements have been carried out at zero and non-zero magnetic field. Obtained absolute Nusselt number turns out to be rather independent from dissipated electric power of the heater 5, 10 and 15 W. Obtained results are shown in Table 2. The second column of the Table 2 displays velocity of the working liquid around the heater, calculated by Eq. (8). For the corrected main velocity (the third column) the diminution of cross-section of the cell due to the heater body is taken into account: from the flow continuity $s{\cdot}u = const$ one should reduce the velocity away from the heater by a proportion of corresponding gap widths (mm): $(15 - 4)/15$.

5. Discussion

The main subject of discussion is the accordance between results of numerical simulation and experimental work, which turns out to be rather good. Let us compare numerically simulated Fig. 7a and b with experimentally obtained Figs. 9 and 10. The effect that lower temperature difference gives more magnetic intensification related to zero field experiments, is shown in Fig. 7a with Nu/Nu_0 as well as in Fig. 9 with α/α_0 (the case $h' = 0$). For the case $h' = 0$ Fig. 7 gives the increment of intensification of ~4% with respect to changing ΔT from 20 to 15 K. From experimental results (Fig. 9) one obtain ~5% at the warm end and 1–2% at the cold end. These results seem to be correct by taking into account nonsymmetrical heat loss through the sidewalls of the cell.

Second point is to compare Fig. 7b with Fig. 10. Numerical simulation gives the relation Nu/Nu_0 vs. the magnet shift h' (mm) to be quite constant within the range $-20 < h' < 0$ and equal to -0.05 mm^{-1}. Experiment provides with α/α_0 vs. the magnet shift h' that also is rather constant from -20 mm up to at least 0 mm, and farther up to 20 mm only a little less. Paying attention to the range -20 to 0 mm, experimentally obtained slopes α/α_0 vs. h' (mm) are -0.13 mm^{-1} at the warm end and -0.03 mm^{-1} at the cold end. As in the first comparison, the numerical estimation is between experimental ones at both ends. Although, quantitatively in the experiment the warm end exhibits 2–3 times larger sensitivity to the magnet shift than the numerical estimation. The main reason may be that theoretical model deals with simplified configuration of the magnetic field, moreover, β_T is ignored in the magnetic Rayleigh number Rm. That causes a larger discrepancy with taking the magnetic field nearer to the heater.

At the end, the value of averaged vertical velocity can be compared. The result of numerical simulation is 21 mm s^{-1} with the magnet position $h' = 0$ (Fig. 4). Table 2 gives for that case the corrected main velocity 20 ± 2 mm s^{-1}. Perfect accordance in such a complicated both simulation and experiment might be taken partly as an occasion, but as a matter of fact, the accordance in this point is primely proved.

6. Conclusions

In a convection cell with attached permanent magnets the thermomagnetic convection may exceed that of thermogravitational

Table 2
Obtained averaged between the separating ribs vertical flow velocity (estimated accuracy ±2 mm s^{-1}).

Experimental conditions	Velocity along the heater (mm s^{-1})	Corrected main velocity (mm s^{-1})
Zero-field experiment	12	9
Magnet position $h' = 0$ mm	27	20
Magnet position $h' = -20$ mm	38	28

many times. Efficiency of the thermomagnetic convection depends on placement of magnets with respect to warm and cold ends of the cell. Maximal thermomagnetic intensification is achieved when magnets are placed as near as possible to the warm (cooled) end.

Comparision between numerically simulated and experimentally obtained results proves to be quite successful. Results are compared in three aspects: magnetic intensification as dependent on the temperature difference, on the magnet shift, and averaged vertical flow velocity. The accordance varies from perfect to 2–3 times quantitatively. In fact, the accordance between derivatives of magnetic intensification on the temperature difference and on the magnet shift cannot be given precisely. Due to technical reasons the experiment provides short range of changing parameters, so the accuracy of obtaining derivatives is of the same order as comparison with the numerical results.

The applying of surface cooling based on the thermomagnetic convection in technical use is under the question. Reached with the present setup the cooling effect of 0.075 W cm^{-2} seems to meet only low technical demands. The present work proves the finding of Rosensweig [19] that a significant augment of the cooling intensity by thermomagnetic convection can be obtained only in a case if the heat source is located into the region of a maximal magnetic field intensity, when the efficiency of power generation cycle reaches its maximum.

References

[1] E. Blums, A. Cebers, M.M. Maiorov, Magnetic Fluids, Walter de Gryuter, Berlin, 1997.
[2] B.A. Finlayson, Convective instability of ferromagnetic fluids, J. Fluid Mech. 40 (4) (1970) 753.
[3] M.S. Krakov, I.V. Nikiforov, To the influence of uniform magnetic field on thermomagnetic convection in square cavity, J. Magn. Magn. Mater. 252 (2002) 209–211.
[4] A. Lange, Thermal convection of magnetic fluids in a cylindrical geometry, J. Magn. Magn. Mater. 252 (2002) 194–196.
[5] E. Blums, A. Mezulis, G. Kronkalns, Magnetoconvective heat transfer from a cylinder under the influence of a nonuniform magnetic field, J. Phys.: Condens. Matter 20 (20) (2008).
[6] D. Zablockis, V. Frishfelds, E. Blums, Numerical investigation of thermomagnetic convection in a heated cylinder under the magnetic field of a solenoid, J. Phys.: Condens. Matter 20 (20) (2008).
[7] M.S. Krakov, I.V. Nikiforov, A.G. Reks, Influence of the uniform magnetic field on natural convection in cubic enclosure: experiment and numerical simulation, J. Magn. Magn. Mater. 289 (2005) 272–274.
[8] H. Yamaguchi, Z. Zhang, S. Shuchi, K. Shimada, Heat transfer characteristics of magnetic fluid in a partitioned rectangular box, J. Magn. Magn. Mater. 252 (2002) 203–205.
[9] T. Sawada, H. Kikura, T. Tanahashi, Visualization of wall temperature distribution caused by natural convection of magnetic fluids in a cubic enclosure, Int. J. Appl. Electromagn. Mater. 4 (4) (1994) 329–335.
[10] R. Ganguly, S. Sen, I.K. Puri, Heat transfer augmentation using a magnetic fluid under the influence of a line dipole, J. Magn. Magn. Mater. 271 (1) (2004) 63–73.
[11] K. Nakatsuka, B. Jeyadevan, S. Neveu, H. Koganezawa, The magnetic fluid for heat transfer applications, J. Magn. Magn. Mater. 252 (2002) 360–362.
[12] H. Yamaguchi, A. Sumiji, S. Shuchi, T. Yonemura, Characteristics of thermomagnetic driven motor using magnetic fluid, J. Magn. Magn. Mater. 272-276 (3) (2004) 2362–2364.
[13] F. Koji, Y. Hideaki, I. Masahiro, A mini heat transport device based on thermosensitive magnetic fluid, Nanoscale Microscale Thermophys. Eng. 11 (1) (2007) 201–210.
[14] Q. Li, W. Lian, H. Sun, Y. Xuan, Investigation on operational characteristics of a miniature automatic cooling device, Int. J. Heat Mass Transfer 51 (21) (2008) 5033–5039.
[15] W. Lian, Y. Xuan, Q. Li, Characterization of miniature automatic energy transport devices based on the thermomagnetic effect, Energy Convers. Manage. 50 (1) (2009) 35–42.
[16] M. Maiorov, E. Blums, H. Hanson, C. Johanson, High field magnetization of the colloidal Mn–Zn ferrite, J. Magn. Magn. Mater. 85 (1990) 129–132.
[17] S.M. Snyder, T. Cader, B.A. Finlayson, Finite element model of magnetoconvection of a ferrofluid, J. Magn. Magn. Mater. 262 (2) (2003) 269–279.
[18] V.P. Isachenko, V.A. Osipova, A.S. Sukomel, Teploperedacha (in Russian), Energiya, Moskva-Leningrad, 1965.
[19] R.E. Rosensweig, Ferrohydrodynamics, Cambridge University Press, Cambridge, MA, 1985. 344 pp..

III Apakšvirziens

Degšanas procesu dinamikas izpēte.

Eksperimentālās iekārtas:

Magnētiskā lauka un liesmas virpuļplūsmas mijiedarbības eksperimentālie pētījumi:
1. Iekārta ar pastāvīgo četrpolu magnētu:

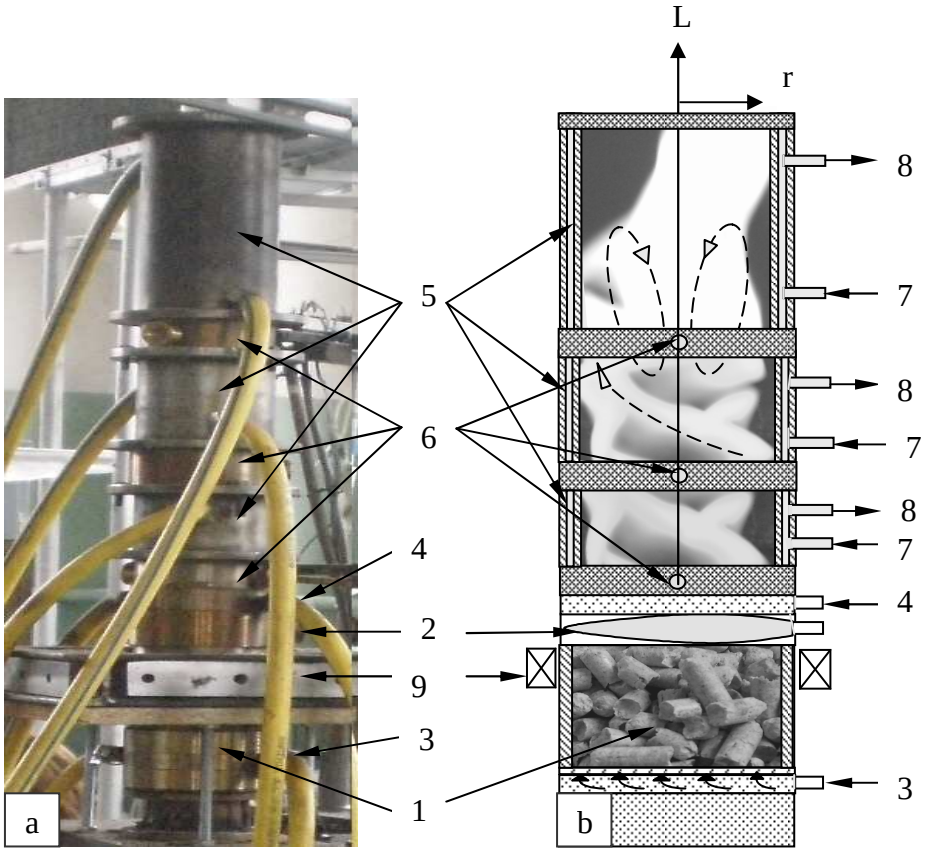

Eksperimentālās iekārta pastāvīga magnētiskā lauka un liesmas virpuļplūsmas mijiedarbības eksperimentālajiem pētījumiem atjaunojamā kurināmā degšanas procesā; 1- koksnes gazifikātors; 2- propāna deglis kombinētā degšanas procesa izveidei; 3.- primārā gaisa padeves sprausla; 4.- tangenciālā sekundārā gaisa padeve; 5.- dzesējamā sekcionēta degšanas kamera gaistošo savienojumu sadedzināšanai; 6.- diagnostikas sekcijas liesmas virpuļplūsmas temperatūras, ātruma un sastāva lokāliem mērījumiem; 7., 8.- dzesējamā ūdens padeve kalorimetriskiem saražotā siltuma daudzuma mērījumiem dažādās degšanas procesa attīstības stadijās; 9. – četru polu pastāvīgais magnēts liesmas un magnētiskā lauka mijiedarbības eksperimentālajiem pētījumiem.

2. iekārta ar elektromagnētu:

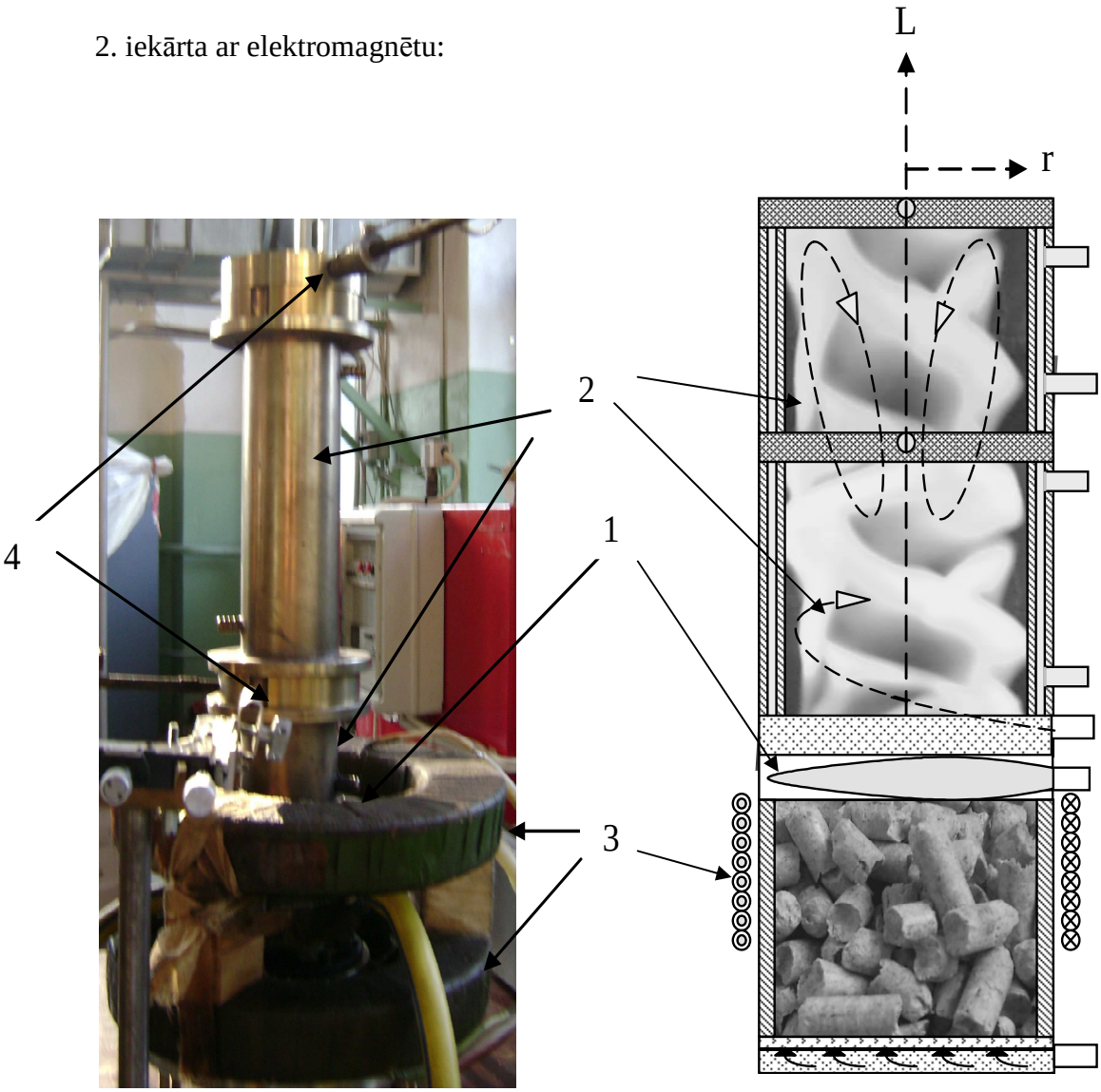

Eksperimentālās iekārta maināma magnētiskā lauka un liesmas virpuļplūsmas mijiedarbības eksperimentālajiem pētījumiem atjaunojamā kurināmā degšanas procesā; 1- propāna deglis, 2- dzesējamā degšanas kamera; 3 - elektromagnēts; 4- diagnostikas sekcijas.

Eksperimentālās iekārtas dažādu struktūru atjaunojamā kurināmā degšanas procesu pētījumiem (sadarbība ar VKĶI):

1. Mazas jaudas eksperimentālā iekārta dažādu struktūru granulēta lignīna degšanas procesu pētījumiem:

Eksperimentālās iekārtas digitālais foto

Granulētais salmu un koksnes lignīns

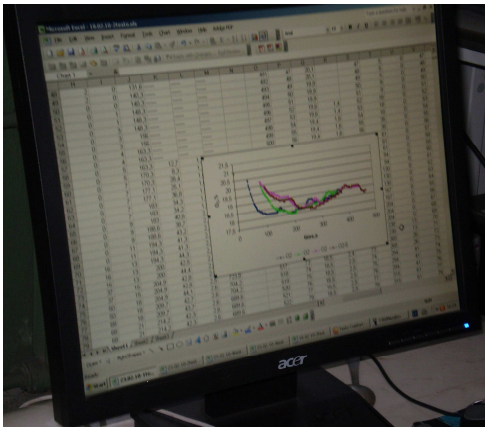

Degšanas produktu sastāva datorizētā reģistrācija

2. Eksperimentālais katls gāzveida kurināmā un dažādu struktūru atjaunojamā kurināmā līdzsadedzināšanai (patents):

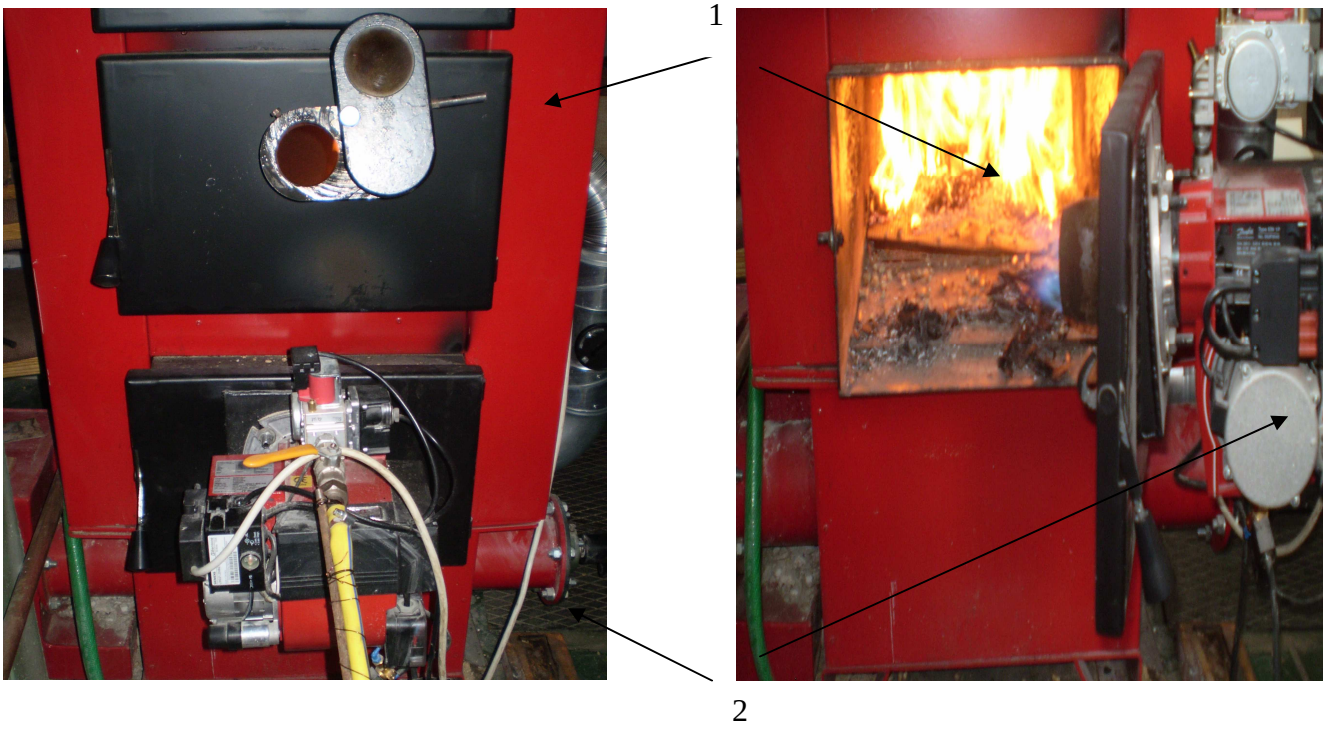

Eksperimentālais katls; 1- kurtuve; gāzes deglis